Stochastic foraging paths primarily drives within-species variations of prey consumption rates

Vincent Bansaye, Geoffroy Berthelot, Amina El Bachari, Jean-René Chazottes, Sylvain Billiard

Stochastic foraging paths primarily drives within-species variations of prey consumption rates

Vincent Bansaye[a], Geoffroy Berthelot[a,b,c], Amina El Bachari[a], Jean-René Chazottes[d], and Sylvain Billiard[e,1]

[a]Centre de Mathématiques Appliquées (CMAP), CNRS, Ecole polytechnique, Institut Polytechnique de Paris, Palaiseau, France; [b]Institut National du Sport, de l'Expertise et de la Performance (INSEP), Paris 75012, France; [c]Research Laboratory for Interdisciplinary Studies (RELAIS), Paris 75012, France; [d]Centre de Physique Théorique, CNRS, Ecole polytechnique, Institut Polytechnique de Paris, Palaiseau, France; [e]Univ. Lille, CNRS, UMR 8198 – Evo-Eco-Paleo, F-59000 Lille, France

This manuscript was compiled on May 29, 2024

The speed at which individuals interact, in particular prey and predators, affects ecological processes at all scales, including how fast matter and energy flow through ecosystems, and how stable communities are. Environmental heterogeneity and individual variabilities are generally believed to be the main factors underlying the variation of consumption rates of prey by predators. We challenge this view by comparing predicted variability from a stochastic model to experimental data. We first analyze a stochastic model of a simple random walk with elementary ecological processes involved in prey consumption, including prey depletion, predator movements and prey handling. We provide sharp approximations of the distribution of the consumption rate and a quantitative prediction of the coefficient of variation when stochastic foraging is the only source of variability. Predictions are then compared to the coefficients of variation estimated from data from dozens of various species and experimental contexts. We show that the predictions only accounting for intrinsic stochasticity in foraging are compatible with the range of observed values, in particular in 1 or 2 dimensional space. After evaluating the robustness of our model's predictions through stochastic computer simulations, we conclude that the main driver of the variation of the consumption rate is the foraging process itself rather than environmental or between-individual variabilities. Our approach lays the foundations for unifying foraging theory and population ecology, and as such has many empirical and theoretical implications for both fields.

The assessment of ecosystems services, of the impact of harvesting natural resources, or of the stability of ecological communities requires identifying the main drivers of biomass and energy flux and species dynamics. In particular, the consumption rate of prey at different levels of trophic food webs, such as prey by predators, affects the dynamics of ecological networks (e.g. plant-insects (1)), or the evolution of traits involved in interactions, as between hosts and their parasites (2). Decades of researches in ecology provided a vast catalog of possible factors affecting the variability of consumption rates within and across species, suggesting consumption rates are idiosyncratic and their variability is due to specificity at different scales, from the contingent evolutionary history of each species (3) to individuals' personality, experience or ontogeny (4–7). Here, we challenge this view and test the hypothesis that observed within-species variations in consumption rates were mostly due to the intrinsic stochasticity of foraging in a depleted, unknown and spatialized environment.

Many factors have been identified as potential drivers of the variations of the consumption rates in predator-prey interactions, as testifies the abundant literature studying the evolution of traits and behaviors involved in foraging or the functional form of the relationship between prey abundance and predator consumption rates (the so-called functional responses). For instance, the time devoted to search for a prey depends on its local density (8–10), on the seasonal or spatial variation of the habitat (11, 12), the heterogeneity of prey distribution (13–15), the dimensionality of the environment (16–18), the presence of competing foragers (19) or the relative size between the prey and the predator (20, 21). Once a prey is found, the predator must spend some time to handle it which might depend on the quality of the prey (22) or on where and when it is more efficient to forage for another prey (23). Any other kind of interactions within or between species can also affect the consumption rates: predators can change their behavior in response to their own predators (24, 25), because of parasitism (26), if foraging is collective (27), or the rate at which prey are regenerated (28, 29).

A majority of studies have focused on a single factor among many others, in one or a few species. A few large scale analyses assessed whether one or several of these factors would drive variability of the consumption rates both within and between species. (30) showed that body mass and environment temperature generally affect the mean consumption rate across species. (31) focused on systematic statistical biases due to the non-linearity of the functions that are inferred in population ecology, casting doubt on estimations and models comparison, but also highlighting that experimental and methodological errors should be accounted for. All studies considered only three possible sources of variations (environmental, between-individuals or measurement errors), but did not consider variation that could come from the foraging process itself. Considering that foraging is a stochastic process in an unknown and depleted environment, the stochasticity of the foraging process itself is an unavoidable intrinsic source of variation of the consumption rate of prey by predators. Even if experimental conditions are perfectly controlled, if individuals are identical and if there are no measurements errors, foraging individuals would follow different paths when searching for prey, producing an intrinsic source of variation.

Our goal is to theoretically quantify this intrinsic source of variation and to compare it to experimental data. In the end, we aim at addressing the following questions: are observed variations of the same order of magnitude than the variations expected under stochastic foraging only? If so, that would suggest that environmental heterogeneity, between-individuals variability

or measurements errors have negligible effect on a large scale on the variation of the consumption rates. Otherwise, if the observed variations are much larger than expected under foraging stochasticity only, that would be an evidence that these other sources of variability are the primary drivers. Finally, if observed variations are much smaller than expected, that would be evidence that some additional behavioral or ecological mechanisms are central. Our approach thus overall consists in providing predictions under a stochastic 'null' or 'neutral' model and evaluate to what extent it can explain the variability observed in data.

To this end, we derive the distribution of consumption rates that describes the number of prey consumed over a given foraging duration by a single predator modeled as a random walk, taking into account dimensionality, prey depletion, and handling and searching times. Although random walks are well-known objects extensively studied in mathematics and physics, their connection to consumption rates and functional responses in ecology has not yet been explored. We find sharp approximations of the distributions of the consumption rate by exploiting duality identities between a simple random walk and the foraging process. We then estimate the asymptotic of the range and the return times of a random walk, and we use uniform integrability via exponential moments to quantitatively predict the coefficient of variation, which is a standardized statistic measuring the relative magnitude of variations. We then compare the theoretical coefficient of variation of the consumption rates to the ones obtained in experimental and field observations. With numerical simulations, we then assess the generality or our results by estimating the robustness of the theoretical coefficient of variation. Our results suggest that the intrinsic stochasticity of the foraging process is the main driver of consumption rates variation, because predators visit already depleted sites a large proportion of their foraging time.

Distribution of the consumption rate in a spatialized depleted environment

Our first goal was to quantitatively evaluate the order of magnitude of the variations of the consumption rates due to the stochasticity of the foraging process itself, while neglecting all other possible sources of variations (between-individual and environmental variabilities, measurements errors). We developed a stochastic model containing the simplest yet most fundamental mechanisms shared by predator species: predators forage in an unknown spatialized environment; they take some time to consume prey; their prey are depleted when consumed; and their total foraging duration is large relatively to moving from one site to another and handling a prey. We considered one predator following a symmetrical random walk on a regular grid, either in 1d, 2d or 3d, during a total duration t. Even though these assumptions are very simple, they are satisfied when the scale of movements are large enough relatively to body size and foraging bout duration (3). Each node initially contains a prey with probability p. The predator has no memory of its past foraging path and prey do not regenerate. The searching time τ_e, i.e. the time taken by the predator to move from one site to another, only depends on the distance between sites. If the predator visits a site containing a prey, it spends there a time τ_h (the handling time) to consume the prey before moving to another site. If the site is empty, the predator randomly and immediately moves to one adjacent site. As the foraging path followed by the predator is stochastic, the total number of prey R_t consumed during the foraging bout with duration t is a random variable, as well as the consumption rate $F_t := R_t/t$. Assuming the duration of foraging t is large, the distribution of $F_t^{(d)}$ in a d-dimension space can be approximated by (proofs in Supp. Mat. A and B)

$$\begin{cases} F_t^{(1)} = \frac{p}{\sqrt{t\tau_e}}\mathcal{W}_t^{(1)} + o_{\mathbb{P}}\left(\frac{1}{\sqrt{t}}\right), \\ F_t^{(2)} = \frac{p\pi}{\tau_e \ln\frac{t}{\tau_e}}\left(1 - \frac{1}{\ln\frac{t}{\tau_e}}\left(\gamma + \pi\frac{\tau_h}{\tau_e} + 2\pi\mathcal{W}_t^{(2)}\right)\right) + o_{\mathbb{P}}\left(\frac{1}{(\ln t)^2}\right), \\ F_t^{(3)} = p\left(\frac{\kappa}{\tau_e+\kappa\tau_h} + \sqrt{\frac{\ln\frac{t}{\tau_e}}{t\tau_e\left(1+\kappa\frac{\tau_h}{\tau_e}\right)^3}}\mathcal{W}_t^{(3)}\right) + o_{\mathbb{P}}\left(\sqrt{\frac{\ln t}{t}}\right), \end{cases} \quad [1]$$

where K, κ, γ and π are numerical constant with known explicit values, $\mathcal{W}_t^{(d)}$ are random variables whose law only depends on dimension $d = 1, 2, 3$, $o_{\mathbb{P}}(\eta_t)$ means that the quantity is negligible compared to η_t in probability, *i.e.* for any $\varepsilon > 0$, $\mathbb{P}(o_{\mathbb{P}}(\eta_t) \geq \varepsilon\eta_t) \to 0$ as $t \to \infty$. Eq. (1) shows that, depending both on the dimension of prey distribution in space and on the predator's movements, the consumption rates follow different distributions $\mathcal{W}_t^{(d)} =_{\text{law}} \mathcal{W}^{(d)}$. This is because the foraging path itself has very different properties: $\mathcal{W}^{(1)}$ is the difference between the maximal and minimal position of a 1-dimensional Brownian motion; $\mathcal{W}^{(2)}$ is the local time of self-intersection of a 2-dimensional Brownian motion; $\mathcal{W}^{(3)}$ is a centered Gaussian distribution. Despite the simplicity of the process, only accounting for spatial structure, depletion, searching and handling, it gives rise to rich and non-trivial emerging properties: the form of the first order of the distribution approximation (the deterministic part) strongly depends on dimension: handling has no role in 1d, only a second order role in 2d, and a first order role in 3d. Eq. (1) also shows that the second order term, that reflects the magnitude of random fluctuations, can not be neglected in 1d or 2d as its magnitude is equal or similar to the first order term (the mean). In addition, stochastic fluctuations in 1d or 2d follow non-classical distributions. In a 3d environment, the random fluctuations of the consumption

VB, SB and JRC designed and supervised the study. GB ran the simulations and produced the associated appendix and figures. SB collected and analyzed data. SB wrote the first version of the paper. SB, VB, GB, and JRC revised the paper until its final version. VB and JRC proved the theorems. AEB participated in extending the model for including initial heterogeneity in the distribution of prey.

The authors declare no conflicts of interest.

[1] To whom correspondence should be addressed. E-mail: sylvain.billiard@univ-lille.fr

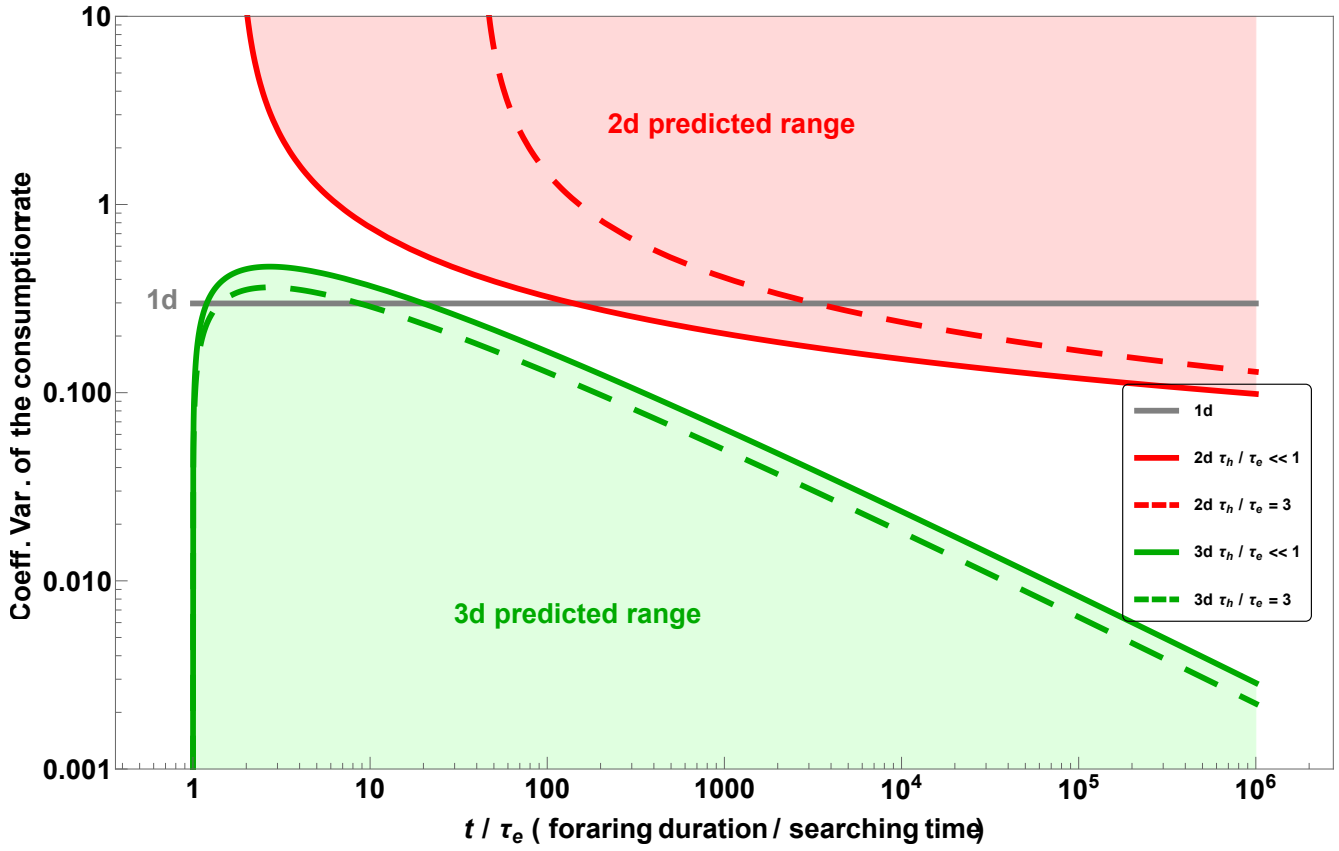

Fig. 1. Predicted range of the coefficient of variation of the consumption rate in a simple random walk with handling (Eq. (2)). Solid lines (no handling time, $\tau_h = 0$): minimum coefficient of variation in 2d (red solid line); maximum coefficient of variation in 3d (green solid line). Solid gray line: coefficient of variation in 1d (independent of the total foraging time t, foraging time between sites τ_e and handling time τ_h).

rate are expected to have a much smaller magnitude than the mean, and to follow a Gaussian distribution with a non-standard normalization.

Coefficient of variation of the consumption rates due to foraging

Our goal is to evaluate the contribution of the intrinsic stochasticity of foraging on the within-species variation of consumption rates across all species and observational contexts. We thus chose the coefficient of variation as a standardized statistic for measuring the variability of the consumption rates. The expected coefficient of variation of the consumption rates under foraging stochasticity was calculated from the two first moments of the distribution of the consumption rate as $\mathrm{CV}_t^{(d)} = \sigma\left[F_t^{(d)}\right] / \mathbb{E}\left[F_t^{(d)}\right]$, where $\mathbb{E}$ and σ respectively are the mean and standard deviation. When the duration of foraging t is large, the coefficient of variation can be approximated for $t \to \infty$ by (Eq. (1), Supp. Mat. B)

$$\mathrm{CV}_t^{(d)} \simeq \begin{cases} \sqrt{\frac{\pi}{2}\ln 2 - 1} \approx 0.298, & d = 1 \\ \frac{\sqrt{2K}}{\ln\frac{t}{\tau_e} - \gamma - \pi\frac{\tau_h}{\tau_e}}, & d = 2 \\ \frac{3}{\pi}\sqrt{\frac{3}{2}}\frac{\kappa}{\sqrt{1+\kappa\frac{\tau_h}{\tau_e}}}\sqrt{\frac{\ln\frac{t}{\tau_e}}{\frac{t}{\tau_e}}}, & d = 3. \end{cases} \quad [2]$$

Our model predicts that the coefficient of variation of the consumption rate covers a very large range of orders of magnitude, but neither for all dimensions nor all parameter values (compare the green and red zones, and the gray line in Fig. 1). Roughly speaking (see also Mat. and Met.), the coefficient of variation should be of order 10^{-1} in 1d, at least of order 10^{-1} in 2d, and at most of order 10^{-1} in 3d. Under the assumptions that the searching time of sites with potential prey is much lower than the total foraging duration ($t/\tau_e \gg 1$, e.g. (24, 32)) and that the handing time is at most of the same order than the searching time ($\tau_h/\tau_e \sim O(1)$, e.g. (24, 30, 32)), the coefficient of variation when considering the stochasticity of foraging only, can even further be expected to be almost constant and lie between orders 10^{-1} and 1 in 1d and 2d, or to be very small ($\ll 10^{-1}$) in 3d (Fig. 1) .

Predicted vs. observed coefficients of variation

In order to test to what extent the stochasticity of foraging on its own drives the variability of the consumption rates, we compared our model's quantitative predictions to coefficients of variation estimated from data. The consumption rates were collected from three categories of datasets, with different uncertainty levels and experimental controls, and different potential sources of variations (see Methods and Supp. Mat. E for further details). Dataset 1: the highest level of uncertainty as it largely comes from the automatic digitization from figures and tables in published papers. Dataset 2: an intermediate level of uncertainty as it was not known whether a single individual was used different times for a given or different treatments, which made not possible the distinction between within and between-individuals variability. Dataset 3: the lowest uncertainty as the observed individuals were known and observed several times. We then calculated the coefficient of variation of the foraging rates for all datasets for each experimental treatments (i.e. generally for an environmental condition, a given pair of prey and predator species, and a given initial prey density). We obtained more than 3800 estimations of the coefficient of variation, for more than one hundred species of prey and one hundred species of predators, for species ranging from unicellular (e.g. ciliates) to vertebrate (e.g. fish and birds), for initial prey density varying by up to 15 orders of magnitude across experiments. We then compared the range of observed values with the expected values under foraging stochasticity only (Fig. 2, Fig. Supp E.1). For all three datasets, a large majority of the measured coefficients of variation lie between 0.1 and 1 (respectively 73.2%, 87.8% and 85.1% for datasets 1, 2 and 3; Fig. 2(a-c), Fig. Supp E.1). The medians are close to 0.298, the value predicted in 1d (respectively 0.291, 0.408 and 0.273). In a large majority of cases, the observed coefficients of variation falls within the range predicted in our model in a 1d or 2d environment. In addition, the predicted range of the coefficients of variation in 2d is in line with a larger proportion of observations than in 3d for all three datasets (85.2% vs. 69.3%, 92.3% vs. 60.3%, and 86.9% vs. 75.5%, 2d vs. 3d, in datasets 1, 2 and 3, respectively). It suggests that foraging effectively occurred as in a 1d or 2d space. Figure 2(a-b) also shows that the dimensionality of the experiment has no effect on the range of the observed coefficients of variation, as the observed coefficients of variation cover the whole range of predicted values (compare colored dots in Fig. 2(a) and (b)).

We then assessed the validity and robustness of the predicted coefficient of variation using numerical stochastic simulations by accounting for additional ecological mechanisms possibly adopted by different species: memory, preferred foraging direction and larger movements. Fig. 3 (a) shows that the coefficient of variation predicted in our model is very close to simulations in 1d, but it is slightly overestimated in 2d and 3d (predicted and simulated values are yet of similar order of magnitude). This overestimation might be due to a very slow speed of convergence of the approximation as the predicted values slightly gets closer to simulations when times t increases (Fig. 3 (a)). As predicted by our model (Eq. (2)), the probability p that a site initially contains a prey does not affect the coefficient of variation (Fig. 3(b)). Short term memory slightly decreases the coefficient of variation (compare Figs. 3(a) and (c)). Longer movements significantly decrease the coefficient of variation in 2d but only when the jump range is very large (dark dots), otherwise they do not affect it in 1d and only slightly in 3d (Fig. 3(d)). Finally, the coefficient of variation is strongly affected when the predator has a preferred foraging direction, which is not surprising as the foraging path becomes more deterministic as the weight of direction preference increases (Fig. 3(e)). Overall, we found that our model is robust to additional mechanisms except in situations where the stochasticity of the foraging paths is decreased. This is consistent with general properties of random walks (see Supp. Mat. A4). Hence, additional mechanisms can, on the one hand, have little effect on the coefficient of variation which would explain why most observed values fall in the range predicted by our model (between 0.1 and 1). On the other hand, they can partly explain why observed coefficients of variation are much lower than 0.1.

Searching for prey is the main driver of consumption rate variability

In summary, despite several sources of variations in experiments could contribute to the estimated coefficient of variations, stochasticity of the foraging process alone is quantitatively compatible with the range covered by data. Two possibilities can explain that the coefficients of variation estimated from observations mostly lie between 0.1 and 1 across a large majority of species and observational contexts (Fig. 2, Supp. Inf. C)). *Hypothesis 1*: Foraging paths stochasticity is negligible relatively to other sources of variability. If so, one should explain how is it possible that between-individual variability, environment heterogeneity and measurements altogether scale such that the estimated coefficients of variation mostly varies in such a small range of values between (0.1-1) across all species and experimental contexts. *Hypothesis 2*: Foraging paths stochasticity is the main driver, and the effective dimension of foraging is 1d or 2d. As our model's predictions are in line with most of the estimated coefficients of variations, it suggests that experimental errors, environmental and between-individuals variabilities are negligible. In other words, the coefficient of variation of the consumption rate is large in 1d and 2d because the randomness of foraging paths is strongly linked to the randomness of the number of prey effectively consumed. In 3d, paths are also highly random but the number of prey consumed is very little affected by the particular trajectory taken by the predator.
Between-individual, between-species, or environmental variabilities can still affect the consumption rates as its mean and variance depend on the handling and searching times (Eqs. (3) and (4)):

$$\mathbb{E}\left[F_t^{(d)}\right] \underset{t\to+\infty}{\sim} \begin{cases} 2p\sqrt{\frac{2}{\pi}}\frac{1}{\sqrt{t\tau_e}}, & d=1, \\ p\frac{\pi}{\tau_e \ln\frac{t}{\tau_e}}\left(1-\frac{\gamma\tau_e+\pi\tau_h}{\tau_e\ln\frac{t}{\tau_e}}\right), & d=2, \\ p\frac{\kappa}{\tau_e+\kappa\tau_h}, & d=3, \end{cases} \quad [3]$$

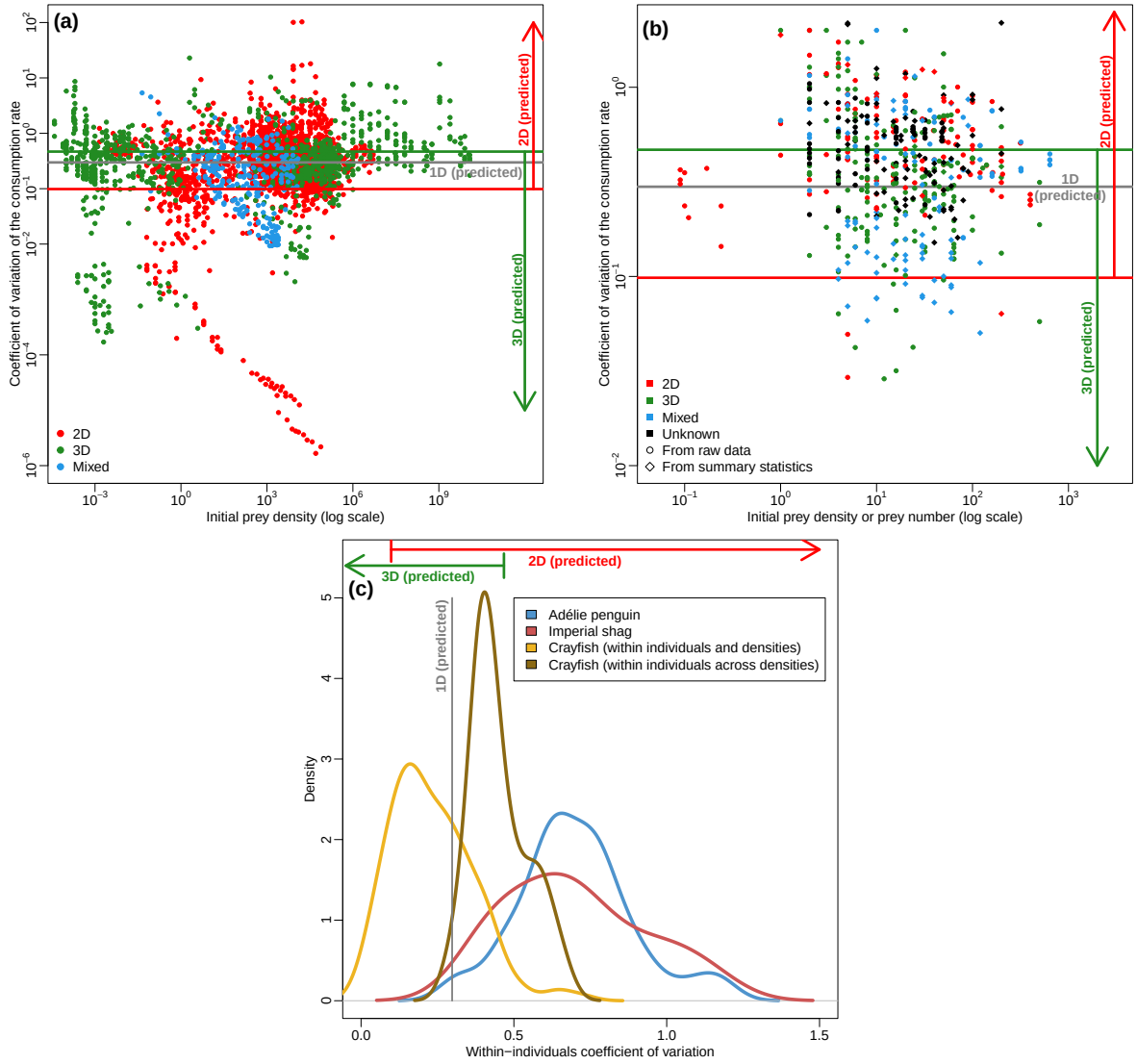

Fig. 2. Coefficients of variation of prey consumption rates in experiments compared to the maximal range predicted by the model (lines). (a) Dataset 1: data from the FoRAGE database; (b) Raw data (between and within individuals variation confounded): (c) Raw data (between and within individuals variation isolated). Dimensionality of space in the model and experiment is represented by colors: Models in 1d, 2d, 3d respectively in black, red and green; Experiments in 2d, 3d or mixed (prey distributed on surfaces in a 3d system, e.g. on leaves in a terrarium) respectively in red, green and blue.

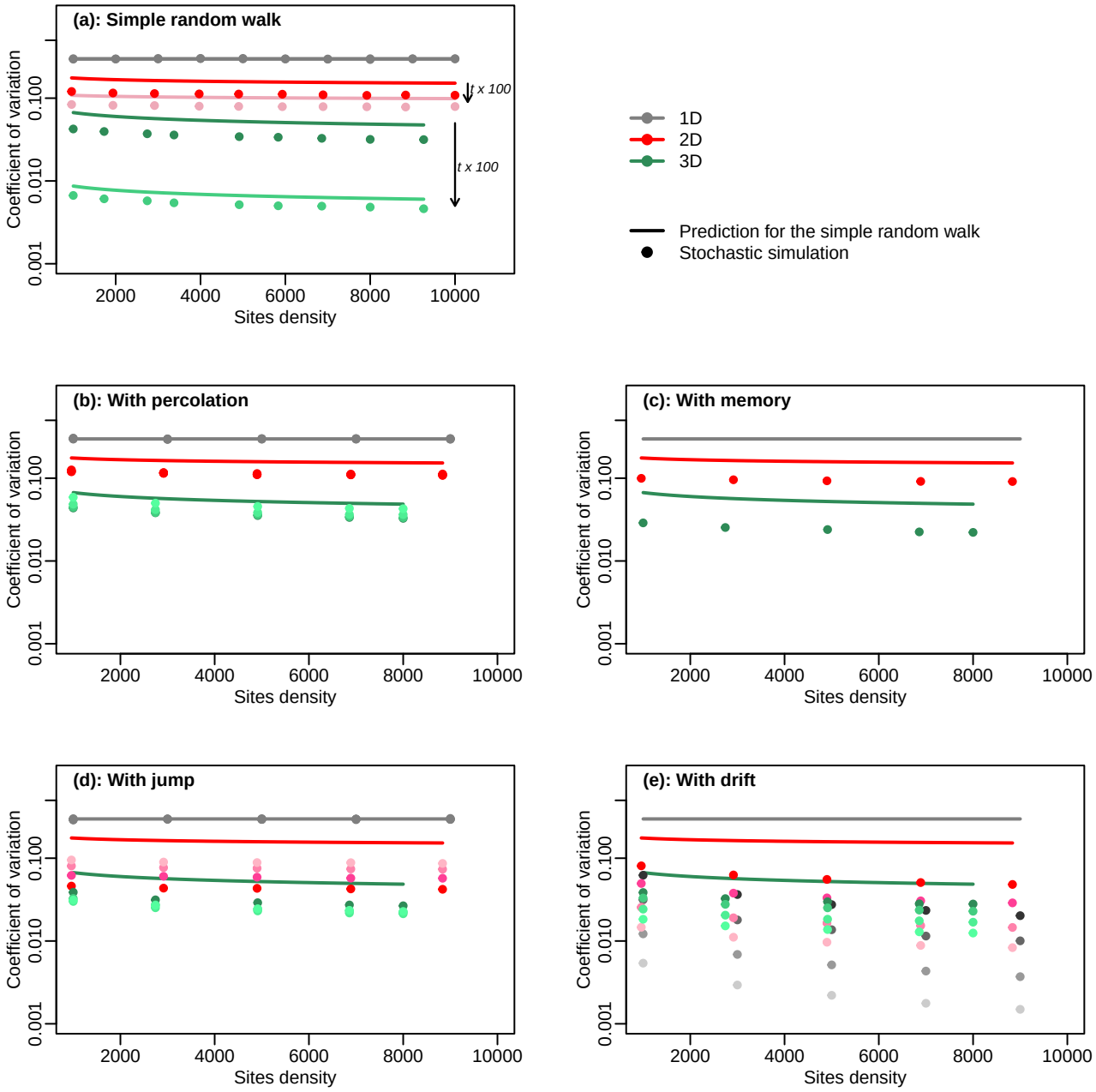

Fig. 3. Robustness of the prediction of the coefficients of variation. The sub-figures compare the value predicted of the coefficient of variation in 1d, 2d or 3d from Eq. (2) (solid line) and the value estimated from exact stochastic simulations (dots) where additional mechanisms are added to the reference model (a) (Eq. (2)) with sites initially containing a prey with probability $p = 0.5$ for two total foraging times $t = 10^5$ and $t = 10^7$; Sub-figure (b) shows coefficients of variation where sites initially contained prey with probability $p = 0.05, 0.1, 0.25, 0.5$ (from darker to lighter colors); (c) With short term memory (the predator avoids the immediate previously visited site); (d) With jump: The predator can move to more distant site in one step. The distance follows a power-law distribution with exponent $\theta = 2, 2.5, 3, 3.5$ (from lighter to darker colors, shorter to larger jumps); (e) With drift: The predator has a preferred foraging direction with weight $\mu = 0.05, 0.1, 0.25, 0.5$ (from darker to lighter colors). Default values for simulations (unless indicated): $t = 10^7, \tau_h = 0.1, \tau_e = L/(x^{1/d} - 1)$ with x the sites density and $L = 10^3$ an arbitrary length value between two sites.

and

$$\mathrm{Var}\left[F_t^{(d)}\right] \underset{t\to+\infty}{\sim} \begin{cases} 4p^2\frac{\ln 2-2/\pi}{t\tau_e}, & d=1, \\ p^2\frac{2K\pi^2}{\tau_e^2(\ln\frac{t}{\tau_e})^4}, & d=2, \\ p^2\frac{27\kappa^4}{2\pi^2}\frac{\ln\frac{t}{\tau_e}}{t(\tau_e+\kappa\tau_h)^3}, & d=3. \end{cases} \quad [4]$$

However, the average of the consumption rate and the magnitude of its fluctuations, measured by the standard deviation, both similarly depend on the parameters of the model in 1d and 2d, in such a way that they are of the same order. In 3d, standard deviations are on the contrary expected to be much smaller than the average. That is why the coefficient of variation is expected to be large for any species or ecological contexts.

Dimensionality matters because of depletion

The mean and variance of $F_t^{(d)}$ are very different depending on dimension (Eq. (3) and Eq. (4)). The relative importance of the searching vs. handling times in a functional response with depletion depends on dimensionality not because of the predator-prey interaction itself (as suggested in (16)), but because the time spent to successfully forage non-empty sites grows on different scales. In 1d, the handling time τ_h is negligible, while in 3d the searching and handling times have an effect of the same order. In 2d, handling has an effect of the same order than searching when foraging duration is short, otherwise it has a second order effect on the consumption rate. Consequently, estimating a parameter such as the handling time would need controlling for the time scale of depletion relatively to foraging duration in experiments. Eq. (3) also shows that the decrease of the consumption rate with foraging duration t depends on dimension: it decreases rapidly in 1d (as $1/\sqrt{t}$), slowly in 2d (as $1/\ln t$) and is constant in 3d (as $\mathbb{E}\left[F_t^{(3)}\right]$ does not depend on t at first order).

Eq. (4) shows that handling time has no effect on the variance of the consumption rate $\mathrm{Var}\left[F_t^{(d)}\right]$ in a 1d or 2d environment, even if the repartition of prey in the environment is initially homogeneous ($p = 1$). In contrast, both handling and searching times equivalently affect it in 3d. It thus suggests that handling would little contribute to variation of the consumption rates in a 1d or 2d depleted environment. Eq. (4) also shows that the size of the fluctuations are differently affected by the foraging duration t: in 1d, fluctuations are expected to have the same order as the mean and standard deviation both decreases as $1/\sqrt{t}$; in 2d, fluctuations are expected to be lower than the mean but of similar order, (the mean decreases as $1/\ln t$ and the standard deviation as $1/(\ln t)^2$; in 3d, fluctuations are expected to be of an order lower than the mean (as the mean does not depend on t while the standard deviation rapidly decreases as $1/\sqrt{t}$). This means that it is expected that variability of consumption rates should be negligible in a 3d environment when compared to the mean, but at least of similar order of magnitude in a 1d or 2d environment.

Bridging the gap between foraging theory and functional responses in ecology

Assuming that the searching time τ_e is a decreasing function of prey density x (*e.g.* $1/x^{(1/d)}$), our model also provides functional responses, i.e. a function describing how consumption rate of a predator is related to prey density (8)(Fig. Supp. C.1). Many functional responses have been proposed under the assumption that prey depletion is negligible (33–35), only a few with prey depletion (29, 36, 37). All functional response models have neglected space, the foraging process and its stochastic nature, thus perpetuating a division between the fields interested either in foraging or functional responses (see (9) for a critical review). Here, by explicitly including the foraging process of prey distributed in space, even though under simplifying assumptions, we contribute in bridging the gap between those two mostly independent fields with promising outcomes. For instance, the form of the functional responses with depletion including the foraging process are very different than the one which is mostly used, the Rogers-Royama equation (29, 36, 37). We also show that in a 3d environment, the first order approximation gives the form of a Holling type II functional response. This suggests that depletion would have little effect on the functional response in cases where prey are distributed in 3d. Finally, as our results show that fluctuations of the consumption rate are of the same order than the average, it suggests that using deterministic models such as the Rogers-Royama equation for interpreting data or estimating parameters is limited.

Another assumption differs between the Rogers-Royama model with prey depletion and ours: they supposed a fixed initial number of prey while we supposed an open-ended environment with virtually no prey limitation. At first sight, supposing a fixed initial number of prey would be closer to experimental design as prey are generally distributed in a closed environment at the start of the experiments. However, data show little relationship between initial density of prey and the coefficient of variation (Fig. 2), as predicted by our model (Eq. (2), Fig. 3). In fact, we collected the coefficients of variation from data only when there was variation in the number of prey consumed, i.e. when $CT > 0$. Cases where $\mathrm{CV} = 0$ were found in data only when the initial number of prey was low, i.e. when for a given initial density all prey were consumed by each predator in all replicates. As the order of magnitude of the estimated coefficient of variation lie within the range predicted by our model, it suggests that as soon as there exists some variation in the number of prey consumed, the prey-predator system works as if in an open-ended space. This should depict experimental conditions where the total duration of the experiment was short enough that prey were not fully depleted, but long enough relatively to the handling and searching times. Finally, despite we do not impose a fixed initial number of prey, the order of magnitude of the variation of the consumption rates is well captured by our model, further strengthening our conclusion that the stochasticity of the foraging paths is the main driver.

Theoretical and empirical implications

The fact that foraging variations are mostly driven by foraging paths stochasticity suggests that the handling time has a negligible effect on consumption rate relative to searching time. This is true for both the coefficient of variation and the expectation (Eq. (3)). It also suggests that the variability of the consumption rate within and between species is little affected by the individuals or species properties such as variation in size or other traits, or trophic levels, and that foraging occurs in an environment with an effective dimension 1d or 2d, even when it is actually in 3d. This can be an evidence that predators actually forage in 1d or 2d (38, 39), or, not exclusively, that prey are distributed in 1d or 2d. Finally, other mechanisms certainly affect the consumption rates as many papers showed how animals tend to change their behavior depending on the prey, habitat, their own state, etc. However, our results show that additional mechanisms have negligible impact on within-species variability compared to the intrinsic variability due to searching for prey.

As the predictions from our model are mostly compatible with data, stochastic foraging in a spatialized and depleted environment could be seen as a null model for consumption rates and functional responses studies. It is important because many studies aim at inferring parameters such as the attack rate from experimental data (24, 29, 30). As the variation of the consumption rate has the same order of magnitude than the mean, it makes inference difficult: the control one might have on the quality of an estimator is limited by the inherent noise from the observed process and its outcomes. This result is also important from both a theoretical and empirical viewpoints, as stochasticity in population biology is generally thought to be important only when population is low (e.g. genetic drift, demographic stochasticity). Our results show that it is generally not the case as stochasticity is expected to be large even in large systems on a short time scale. The resulting implications of the interactions stochasticity on the understanding and modeling of populations and communities dynamics remains an open question. On a side note, our results provide a 'quick and dirty' criterion for evaluating the validity of a stochastic model of foraging or prey consumption of a predator: its coefficient of variation should lie between 10^{-1} and 1, and close to 0.3 on average.

As a null model, our approach can also help explaining the observed discrepancies between data and predictions (Fig. 2) such as why coefficients of variation range from one to (rarely) several orders of magnitude lower than 10^{-1}. Our numerical simulations suggest that some non-exclusive additional mechanisms, such that predator's memory or a preferred foraging direction, can significantly decrease the coefficient of variation. Our model also suggests that in some experimental contexts, the effective dimension of foraging is closer to 3d, or that it could be due to the fast regeneration of prey(34), which would however be inconsistent with most experimental conditions. Finally, it could be due to experimental design itself as the boundaries of the environment can be either attractive (39) or repulsive. Coefficients of variation which range from one to several orders of magnitude larger than 1 can be an evidence that other sources of variation are at least as important as the intrinsic stochasticity of the foraging paths. It can also be due to particular situations in 2d such as a large searching or handling times compared to the total foraging duration (Fig. 1).

Finally, our results have implications for the evolution of foraging and the study of the optimal foraging theory. The fitness of individuals depends on the variance of the parameters of the system (40) but also on the inherent variance of the process itself as shown here. As this variance depends on dimensionality, foraging strategies can be expected to have differently evolved depending on dimensionality, yet independently of spatial heterogeneity. Using simulations of random walk in 2d, (41) predicted that optimal foraging strategies would evolve directional motion (i.e. movements with little turning). However, we showed that a preferred direction for foraging tends to largely decrease the coefficients of variation, which would not be consistent with data. This would surprisingly suggest that species have evolved sub-optimal foraging behaviors, as the observed coefficients of variations are larger than expected under a preferred foraging direction. Otherwise, it more likely suggests that other traits and mechanisms have evolved in order to optimize foraging efficiency in an unknown spatialized environment rather than a preferred direction.

Supporting Information (SI). Supporting information are provided as a separate file.

SI Datasets. Information about data sources and accessibility are given in Supp. Inf. E.

Materials and Methods

Please describe your materials and methods here. This can be more than one paragraph, and may contain subsections and equations as required.

Model. A forager performs a random walk in a d-dimension environment where prey are distributed on a lattice. The time taken to go from one site to another is τ_e. Note that by assuming that the searching time τ_e is proportional to $x^{(-1/d)}$, where x is the density of sites potentially containing prey, our functions $F^{(d)}$ are functional responses, as classically defined. If a site is visited for the first time, it contains a prey with probability p. Consuming the prey takes a handling time τ_h. When a prey is consumed, it is not renewed (the time scale for prey renewal is supposed much larger than the foraging time scale). Given these times, the distribution of R_t, the number of prey consumed after a time t, is linked by a duality argument to the distribution of the minimum number of searching steps needed to consume at least a given number of prey. By exploiting the convergence in law of the distribution of the number of distinct sites visited after a given number of steps (42–44), the distribution of $R_t^{(d)}$ converges in law as $t \to \infty$ to different explicit expressions depending on the dimensionality of the environment (Supp. Mat B). Approximations of the first two moments of $R_t^{(d)}$ are then obtained. Finally, the distribution of the consumption rates and its first two moments are then deduced as $F_t^{(d)} := R_t^{(d)}/t$ (see details in Supp Mat. A and B).

Orders of magnitude of the coefficient of variation. Depending on the dimension, the coefficient of variation is expected to differ in orders of magnitude (Fig. 1, note the log-scale on the y-axis). When the total foraging time t is large enough, the coefficients of variation in a 1d, 2d, 3d depleted environments are respectively expected to be of order $\mathcal{O}(1) \gg \mathcal{O}(1/\ln t) \gg \mathcal{O}(\sqrt{\ln t/t})$. Note that the order of magnitude of the coefficient of variation in a renewed environment is close to the one in a 3d depleted environment: $\mathcal{O}(1/\sqrt{t})$ (34). In other words, in 1d, the coefficient of variation is expected to be constant. As $\ln t/\tau_e$ increases very slowly with t/τ_e, the coefficient of variation in 2d is expected to be of an order of magnitude either slightly lower or larger than in 1d (compare the red zone and the gray line in Fig. 1). On the contrary, the coefficient of variation in 3d is expected to rapidly decrease with t/τ_e and thus to be at least one order of magnitude lower than in 1d and 2d. This is because stochastic fluctuations of the number of prey consumed are generally expected to be much larger in 1d or 2d than in 3d. Eq. (2) also shows how the coefficient of variation of the consumption rate is expected to be affected by the ecological and behavioral parameters. In 1d, the coefficient of variation does not depend on any parameter. In 2d and 3d, the coefficient of variation is not affected by the initial heterogeneity of prey repartition p, while it is affected by the searching and handling times τ_e and τ_h in different ways. An increasing searching time τ_e generally increases the coefficient of variation in 2d and 3d, but has a non-monotonous effect in 3d as it decreases it for low values of t/τ_e. The handling time has opposite effect on the coefficient of variation as it increases it in 2d while it decreases it in 3d (Eq. (2), compare full and dashed lines in Fig. 1). In particular, the coefficient of variation shows a maximal value for $\tau_h = 0$ in 3d, while it can take arbitrarily high values in 2d.

Stochastic numerical simulations of foraging rates. The path followed by a foraging individual was numerically simulated on a d-dimensions lattice where each node initially contains a prey with probability p. The individual moves to the next site, which is randomly chosen with equiprobability among the four nearest (cardinal) ones. The sites are homogeneously distributed with a density x on the lattice. One thousand stochastic simulations are generated for all set of parameters values (sites densities x and total foraging duration t). The empirical distribution of the foraging rates and its expectation were estimated. In order to test for the robustness of the approximations obtained with our model, we added behavioral features: random walk with (stochastic) jumps to distant sites, with preferential direction (drifted random walk), with short-term memory (avoidance of the last visited site).

Datasets. The coefficient of variation of the consumption rate were estimated from three different datasets with different degree of uncertainties regarding the sources of variability (*i.e.* data collection methodology, experimental controls, between-individuals variability, within-individuals variability, controlled or uncontrolled environmental variability, variability due to the foraging process itself). Further details are given in Supp. Mat. E. Dataset 1: We extracted relevant data from the FoRAGE database (45) which compiles functional responses from controlled experiments in the published literature. FoRAGE database was populated by raw data or summary statistics either automatically digitized from articles' figures or gathered from articles' tables. There were often uncertainties about how many actual observations were represented by one dot on figures (several dots overlapped if individuals in a replicate consumed the same number of prey). Another uncertainty source was the standard deviations with zero values, which can either be due to entries errors in the database or because of a true absence of variation. We thus decided to discard all experiments with no variation within an experimental treatment in the database. In order to be conservative and to limit noise due to data collection, we also discarded experiments from the FoRAGE database that do not satisfy the following criteria: (i) at least eight independent measurements for a given experimental treatment and (ii) at least 80% of raw data recognizable from the figures among all replicates for a given treatment. We overall estimated 3181 coefficients of variation for various experimental conditions (regarding prey density, temperature, environmental dimensions, prey and predator species, etc.), for 126 predator and 104 prey species, covering a biomass range of near 7 and 12 orders of magnitude, respectively. We sorted data regarding the dimension of the environment (as acknowledged by the database' authors): 2d, 3d, or a mix between 2d and 3d (for instance when prey were distributed on plant leaves within a 3d space such as a terrarium). Overall, the coefficient of variation calculated from Dataset 1 may come from different sources of variation: measurement errors including populating the database and digitization, between and within individuals variability, the stochastic foraging process itself, controlled or uncontrolled environmental variability. Dataset 2: We estimated 602 coefficients of variation from 41 different raw datasets collected either from the Dryad repository, or the database by (31), or directly from the authors. We only considered datasets with a single species of prey in a given experiment, with known initial prey densities or number, and with replicates within densities. The coefficients of variations were directly calculated from raw data when available, or from the mean, the standard error and the number of replicates otherwise. It was generally not known whether replicates used the same individuals several times independently or not. When the experiments considered different treatments for a given density (e.g. different temperatures or prey size), we calculated the coefficient of variation across treatments. Overall, the coefficient of variation calculated from Dataset 2 potentially comes from different sources of variation: measurement errors, uncontrolled environment variability, between and within individuals variability, or the stochastic foraging process itself. Datasets 3: We estimated 229 within-individuals coefficients of variation from datasets kindly provided by Yuuki Watanabe, Agustina Gómez-Laich and Stefan Linzmaier. In the three cases, several measurements were obtained from the same individuals thus allowing to isolate the within individuals from between-individuals variability. These datasets included the consumption rates observed for several individuals during different sessions of observations for each individual. Overall, the coefficients of variation estimated from Dataset 3 potentially comes from different sources of variation: measurements errors, within individual variability, uncontrolled environmental conditions, and the stochastic foraging process itself.

ACKNOWLEDGMENTS. Kilian Raschel for his help in literature searching for fine estimates of return times to the origin of random walks, Eliza Vergu for helpful discussions, Yuuki Watanabe and Stefan Linzmaier for sharing their raw datasets, Agustina Gómez-Laich for having provided the coefficient of variation from their dataset. The authors acknowledge the support of the "Chaire Modélisation Mathématique et Biodiversité (MMB)" of Veolia Environnement-Ecole Polytechnique-Museum National d'Histoire Naturelle-Fondation X, and of the grant MITI CNRS 80'.

1. Thébault E, Fontaine C (2010) Stability of ecological communities and the architecture of mutualistic and trophic networks. *Science* 329(5993):853–856.
2. Dieckmann U, Metz JA, Sabelis M, Sigmund K (2002) Adaptive dynamics of infectious diseases. *Pursuit of virulence management* pp. 460–463.
3. Pyke GH (2015) Understanding movements of organisms: it's time to abandon the lévy foraging hypothesis. *Methods in Ecology and Evolution* 6(1):1–16.
4. Nilsen EB, Linnell JD, Odden J, Andersen R (2009) Climate, season, and social status modulate the functional response of an efficient stalking predator: the eurasian lynx. *Journal of Animal Ecology* 78(4):741–751.
5. Schröder A, Kalinkat G, Arlinghaus R (2016) Individual variation in functional response parameters is explained by body size but not by behavioural types in a poeciliid fish. *Oecologia* 182(4):1129–1140.

6. Lescroël A, et al. (2019) Evidence of age-related improvement in the foraging efficiency of adélie penguins. *Scientific reports* 9(1):3375.
7. Wilson RP, et al. (2022) Luck and tactics in foraging success: The case of the imperial shag. *Marine Ecology Progress Series* 682:1–12.
8. Holling C (1959) Some characteristics of simple types of predation and parasitism. *Canadian Entomologist* 91:385–398.
9. Abrams PA (1982) Functional responses of optimal foragers. *The American Naturalist* 120(3):382–390.
10. Coblentz KE, Novak M, DeLong JP (2023) Predator feeding rates may often be unsaturated under typical prey densities. *Ecology Letters* 26(2):302–312.
11. Watanabe YY, Ito K, Kokubun N, Takahashi A (2020) Foraging behavior links sea ice to breeding success in antarctic penguins. *Science Advances* 6(26):eaba4828.
12. Mocq J, Soukup PR, Näslund J, Boukal DS (2021) Disentangling the nonlinear effects of habitat complexity on functional responses. *Journal of Animal Ecology* 90(6):1525–1537.
13. Goldbogen JA, et al. (2015) Prey density and distribution drive the three-dimensional foraging strategies of the largest filter feeder. *Functional Ecology* 29(7):951–961.
14. Carroll G, et al. (2017) Hierarchical influences of prey distribution on patterns of prey capture by a marine predator. *Functional Ecology* 31(9):1750–1760.
15. Sutton G, et al. (2020) Multi-predator assemblages, dive type, bathymetry and sex influence foraging success and efficiency in african penguins. *PeerJ* 8:e9380.
16. Pawar S, Dell A, Savage VM (2012) Dimensionality of consumer search space drives trophic interaction strengths. *Nature* 486:486–489.
17. Feng Y, Zhou ZX, An MR, Yu XL, Liu TX (2018) The effects of prey distribution and digestion on functional response of harmonia axyridis (coleoptera: Coccinellidae). *Biological Control* 124:74–81.
18. Fall J, Johannesen E, Englund G, Johansen GO, Fiksen Ø (2021) Predator–prey overlap in three dimensions: cod benefit from capelin coming near the seafloor. *Ecography* 44(5):802–815.
19. Smallegange I, van der Meer J (2010) Testing a stochastic version of the Beddington-DeAngelis functional response in foraging shore crabs. *Marine Biology* 157:1027–1040.
20. Rall BC, et al. (2012) Universal temperature and body-mass scaling of feeding rates. *Philosophical Transactions of the Royal Society B: Biological Sciences* 367(1605):2923–2934.
21. Barrios-O'Neill D, et al. (2016) On the context-dependent scaling of consumer feeding rates. *Ecology Letters* 19(6):668–678.
22. Hammill E, Petchey O, Anholt B (2010) Predator functional response changed by induced defenses in prey. *The American Naturalist* 176:723–731.
23. van Gils JA, et al. (2015) Moving on with foraging theory: incorporating movement decisions into the functional response of a gregarious shorebird. *Journal of Animal Ecology* 84(2):554–564.
24. Baker D, Stillman R, Smith B, Bullock J, Norris K (2010) Vigilance and the functional response of granivorous foragers. *Functional Ecology* 24:1281–1290.
25. Smith JA, Wang Y, Wilmers CC (2015) Top carnivores increase their kill rates on prey as a response to human-induced fear. *Proceedings of the Royal Society B: Biological Sciences* 282(1802):20142711.
26. Toscano B, Newsome B, Griffen B (2014) Parasite modification of predator functional response. *Oecologia* 175:345–352.
27. Zimmermann B, Sand H, Wabakken P, Liberg O, Andreassen HP (2015) Predator-dependent functional response in wolves: From food limitation to surplus killing. *Journal of Animal Ecology* 84(1):102–112.
28. Ruscoe WA, Elkinton JS, Choquenot D, Allen RB (2005) Predation of beech seed by mice: effects of numerical and functional responses. *Journal of Animal Ecology* pp. 1005–1019.
29. Rosenbaum B, Rall BC (2018) Fitting functional responses: Direct parameter estimation by simulating differential equations. *Methods in Ecology and Evolution* 9(10):2076–2090.
30. Uiterwaal SF, DeLong JP (2020) Functional responses are maximized at intermediate temperatures. *Ecology* 101(4):e02975.
31. Novak M, Stouffer DB (2021) Systematic bias in studies of consumer functional responses. *Ecology Letters* 24(3):580–593.
32. Ovadia O, Ziv Y, Abramsky Z, Pinshow B, Kotler BP (2001) Harvest rates and foraging strategies in negev desert gerbils. *Behavioral Ecology* 12(2):219–226.
33. Jeschke J, Kopp M, Tollrian R (2002) Predator functional responses: Discriminating between handling and digesting prey. *Ecological Monographs* 72:95–112.
34. Billiard S, Bansaye V, Chazottes JR (2018) Rejuvenating functional responses with renewal theory. *Journal of The Royal Society Interface* 15(146):20180239.
35. Garay J (2019) Technical review on derivation methods for behavior dependent functional responses. *Community Ecology* 20(1):28–44.
36. Royama T (1971) A comparative study of models for predation and parasitism. *Population Ecology* 13:1–91.
37. Rogers D (1972) Random search and insect population models. *Journal of Animal Ecology* 41:369–383.
38. Bartumeus F, da Luz MGE, Viswanathan GM, Catalan J (2005) Animal search strategies: a quantitative random-walk analysis. *Ecology* 86(11):3078–3087.
39. Uiterwaal SF, Dell AI, DeLong JP (2019) Arena size modulates functional responses via behavioral mechanisms. *Behavioral Ecology* 30(2):483–489.
40. Pyke GH (1984) Optimal foraging theory: a critical review. *Annual review of ecology and systematics* 15(1):523–575.
41. Pyke GH (1978) Are animals efficient harvesters? *Animal Behaviour* 26:241–250.
42. Jain NC, Pruitt WE (1972) The range of random walk in *Proceedings of the Sixth Berkeley Symposium on Mathematical Statistics and Probability (Univ. California, Berkeley, Calif., 1970/1971)*. Vol. 3, pp. 31–50.
43. Feller W (1951) The asymptotic distribution of the range of sums of independent random variables. *The Annals of Mathematical Statistics* pp. 427–432.
44. Dvoretzky A, Erdős P (1951) Some problems on random walk in space in *Proceedings of the second Berkeley symposium on mathematical statistics and probability*. (University of California Press Berkeley and Los Angeles), Vol. 2, pp. 353–368.
45. Uiterwaal SF, Lagerstrom IT, Lyon SR, DeLong JP (2022) Forage database: A compilation of functional responses for consumers and parasitoids. *Ecology* 103(7):e3706.

Supplementary Information for "Stochastic foraging paths primarily drives within-species variations of prey consumption rates"

Vincent Bansaye[a], Geoffroy Berthelot[a,b,c], Amina El Bachari[a], Jean-René Chazottes[d], and Sylvain Billiard[e,1]

[a]Centre de Mathématiques Appliquées (CMAP), CNRS, Ecole polytechnique, Institut Polytechnique de Paris, Palaiseau, France

[b]Institut National du Sport, de l'Expertise et de la Performance (INSEP), Paris 75012, France

[c]Research Laboratory for Interdisciplinary Studies (RELAIS), Paris 75012, France

[d]Centre de Physique Théorique, CNRS, Ecole polytechnique, Institut Polytechnique de Paris, Palaiseau, France

[e]Univ. Lille, CNRS, UMR 8198 – Evo-Eco-Paleo, F-59000 Lille, France

[1]To whom correspondence should be addressed. E-mail: sylvain.billiard@univ-lille.fr

May 29, 2024

A Behaviors of the range of random walks

We first gather various results on the number of distinct sites visited by a simple, symmetric, random walk on $\mathbb{Z}^d$. This random variable is usually called the "range" of the random walk. It is the central quantity to define the "functional response" in our context. We will state known results for any dimension d, with a particular focus on dimensions $d = 1, 2, 3$. It turns out that in $d = 1$ and $d = 2$ the mean number of distinct visited sites grows more slowly than the duration n of the random walk, a consequence of "oversampling" as each site is repeatedly visited while the number of visits grows with n. We in particular show that, even in the simplest situation, rich and diverse behaviors of the random walks emerge according to d. We will indicate below the degree of generality in which the following results remain valid (with slight modifications).

A.1 Setting and two basic results

Let $d \geq 1$ be an integer and denote by $(\mathrm{e}^{(1)}, \ldots, \mathrm{e}^{(d)})$ the canonical basis for the lattice $\mathbb{Z}^d$, so we have $i = (i^{(1)}, \ldots, i^{(d)})$ for $i \in \mathbb{Z}^d$. We call "sites" the elements of $\mathbb{Z}^d$. We focus on $d = 1, 2, 3$. Let $(X_n)_{n\geq 0}$ be the simple symmetric random walk on $\mathbb{Z}^d$ starting from the origin, where $X_n = \big(X_n^{(1)}, \ldots, X_n^{(d)}\big)$ is the position of the random walker at time n on $\mathbb{Z}^d$. This process can be viewed as a Markov chain with state space $\mathbb{Z}^d$, initial state $X_0 = 0 := (0, \ldots, 0)$, and transitions probabilities (for $n \geq 0$)

$$\mathbb{P}\big(X_{n+1} = j \,|X_n = i\,\big) = \frac{1}{2d}$$

if $j - i \in \{\pm \mathrm{e}^{(1)}, \ldots, \pm \mathrm{e}^{(d)}\}$ (that is, if i and j are nearest neighbors), and this transition probability is equal to 0 otherwise. The process $(X_n)_{n\geq 0}$ can also be seen as a sum of a sequence of independent identically distributed random variables. Letting $(\xi_k)_{k\geq 1}$ be a sequence of i.i.d. random variables taking values in $\{\pm \mathrm{e}^{(1)}, \ldots, \pm \mathrm{e}^{(d)}\}$ such that

$$\mathbb{P}\big(\xi_k = \pm \mathrm{e}^{(i)}\big) = \frac{1}{2d}, \quad i = 1, \ldots, d$$

we define

$$X_0 = 0 \quad \text{and} \quad X_i = \sum_{k=1}^{i} \xi_k, \quad i = 1, 2, \ldots.$$

Definition A.1. *The range of the random walk is the sequence of random variables defined by*

$$\mathtt{N}_n = \mathrm{Card}\{X_i : i \leq n\} = \mathrm{Card}\big\{k \in \mathbb{Z}^d : \exists\, i \leq n \textit{ such that } X_i = k\big\},\ n \geq 1.$$

By convention we set $\mathtt{N}_0 = 1$.

Hence, $\mathtt{N}_n$ is the number of distinct sites visited up to time n by the random walk. Note in passing that $(\mathtt{N}_n)_{n\geq 0}$ is a non-Markovian process.

Let

$$\kappa = \kappa(d) = \mathbb{P}(\text{no return to } 0) = \mathbb{P}(\forall n > 0 : X_n \neq 0). \tag{A.1}$$

The first result about the range is a kind of "law of large numbers".

Theorem A.2. *Let $d \geq 1$. Then*

$$\mathbb{P}\left(\frac{\mathtt{N}_n}{n} \xrightarrow[n\to+\infty]{} \kappa(d)\right) = 1. \tag{A.2}$$

It is well known that when $d = 1$ or 2, the walk is recurrent, that is, it visits any site infinitely many times with probability one, hence, in particular, $\kappa(1) = \kappa(2) = 0$. When $d \geq 3$, the random walk is transient, hence $0 < \kappa(3) < 1$. See [1, p. 38] for a proof.

The second basic result about the range tells us that, when $d \geq 2$, $\mathtt{N}_n \underset{n\to+\infty}{\sim} \mathbb{E}(\mathtt{N}_n)$, with probability one.

Theorem A.3. *Let $d \geq 2$. Then*

$$\mathbb{P}\left(\frac{\mathtt{N}_n}{\mathbb{E}(\mathtt{N}_n)} \xrightarrow[n\to+\infty]{} 1\right) = 1. \tag{A.3}$$

See [2] for a proof. Notice that this result is not true for $d = 1$. In that case, we will see that $\mathtt{N}_n / \mathbb{E}(\mathtt{N}_n)$ converges only in law (to some non-degenerate random variable).

A.2 Link with return times to the origin

Let $d \geq 1$. For $j \geq 1$, we define new random variables Υ_j associated to the random walk by

$$\Upsilon_j = \begin{cases} 1 & \text{if the } j\text{-th step hits a new site} \\ 0 & \text{otherwise.} \end{cases}$$

Formally, $\Upsilon_j = \mathbb{1}_{\{X_j \neq X_{j-1}, X_j \neq X_{j-2}, \ldots, X_j \neq X_0 = 0\}}$. Hence we have

$$\mathtt{N}_n = \sum_{j=1}^{n} \Upsilon_j \tag{A.4}$$

since we are exactly counting the total number of distinct visited sites when the random walk made n steps. Next, for $j \geq 2$,

$$\mathbb{E}\big(\Upsilon_j\big) = \mathbb{P}\left(X_j \neq X_i \text{ for } i = 1, \ldots, j-1\right)$$

(we have $\mathbb{E}\big(\Upsilon_1\big) = \mathbb{P}(X_1 \neq X_0) = 1$), that is, $\mathbb{E}\big(\Upsilon_j\big)$ is the probability that the j-th step takes the walk to a non-visited site in any of the preceding $j-1$ steps. The basic but fundamental observation is that

$$\mathbb{E}\big(\Upsilon_j\big) = \mathbb{P}(T_0 > j) = \sum_{k=j+1}^{+\infty} \mathbb{P}(T_0 = k) \tag{A.5}$$

where $T_0 = \inf\{n \geq 1 : X_n = 0\}$, the first time the walk hits the origin. That is, the expected value of Υ_j is exactly the probability that the walk did not come back to the origin in j steps (since it starts at the origin). Hence, in view of (A.4) and (A.5), we have

$$\mathbb{E}(\mathtt{N}_n) = \sum_{j=1}^{n} \mathbb{E}\big(\Upsilon_j\big) = \sum_{j=1}^{n} \mathbb{P}(T_0 > j) = \sum_{j=1}^{n} \sum_{k=j+1}^{+\infty} \mathbb{P}(T_0 = k). \tag{A.6}$$

Hence, we are left to estimate $\mathbb{P}(T_0 = k)$ ($k \in 2\mathbb{N}$) to estimate $\mathbb{E}(\mathtt{N}_n)$. [1]

[1] We let $\mathbb{Z}_+ = \{0, 1, 2, \ldots\}$ be the positive integers including 0, and we will denote by $\mathbb{N} = \{1, 2, \ldots\}$ the set of strictly positive integers.

Remark A.4. *Observe that* $\kappa = \lim_{j\to+\infty} \mathbb{P}(T_0 > j) = \lim_{j\to+\infty} \mathbb{E}\big(\Upsilon_j\big)$ *(see* (A.1)*).*

Remark A.5. *It turns out that* (A.5) *(hence* (A.6)*) is valid for any random walk because it only relies on the fact that the random variables* ξ_k *are independent and identically distributed, which implies that* $(\xi_1, \xi_2, \dots, \xi_j) \overset{\text{law}}{=} (\xi_j, \xi_{j-1}, \dots, \xi_1)$*, for all* $j \geq 1$*. Hence, we can "reverse" (in law) the path of the random walk to get*

$$\begin{aligned}\mathbb{P}(X_j \neq X_{j-1}, X_j \neq X_{j-2}, \dots, X_j \neq X_0 = 0) &= \mathbb{P}(\xi_j \neq 0, \xi_j + \xi_{j-1} \neq 0, \dots, \xi_j + \xi_{j-1} + \cdots + \xi_1 \neq 0)\\ &= \mathbb{P}(\xi_1 \neq 0, \xi_1 + \xi_2 \neq 0, \dots, \xi_1 + \xi_2 + \cdots + \xi_j \neq 0)\\ &= \mathbb{P}(T_0 > j).\end{aligned}$$

A.3 Mean, variance and convergence in law of the range

We deal with the cases $d = 1, 2, 3$, considered separately, since very different behaviors occur.

A.3.1 Case $d = 1$

It is straightforward that

$$\mathtt{N}_n = 1 + \max_{0\leq k\leq n} X_k - \min_{0\leq k\leq n} X_k = 1 + \max\{X_p - X_q : 0 \leq p \leq n, 0 \leq q \leq n\}.$$

One expects that $\mathbb{E}(\mathtt{N}_n) = \mathcal{O}(\sqrt{n}\,)$. In [3] the authors obtain the following *exact* formula:

$$\mathbb{E}(\mathtt{N}_n) = \frac{\binom{2\lfloor \frac{n}{2}\rfloor}{\lfloor \frac{n}{2}\rfloor}}{2^{2\lfloor \frac{n}{2}\rfloor}} \left(n + 2\left\lfloor \tfrac{n}{2}\right\rfloor + 1\right),\ n \geq 1.$$

Stirling approximation $n! \underset{n\to+\infty}{\sim} n^n\, \mathrm{e}^{-n}\, \sqrt{2\pi n}$ yields

$$\mathbb{E}(\mathtt{N}_n) \underset{n\to+\infty}{\sim} \sqrt{\frac{8}{\pi}}\, \sqrt{n}. \tag{A.7}$$

For the variance we have (see [4])

$$\mathrm{Var}(\mathtt{N}_n) \underset{n\to+\infty}{\sim} 4\left(\log 2 - \frac{2}{\pi}\right) n. \tag{A.8}$$

The random variable $\mathtt{N}_n\,/\sqrt{n}$ converges in law to a non-degenerate probability distribution ([5],see also [4]), namely, we have the following result.

Theorem A.6. *We have*

$$\frac{\mathtt{N}_n}{\sqrt{n}} \xrightarrow{\text{law}} \mathcal{F} := \max_{0\leq s\leq 1} \mathcal{B}_s^{(1)} - \min_{0\leq s\leq 1} \mathcal{B}_s^{(1)}, \tag{A.9}$$

where $(\mathcal{B}_s^{(1)})_{s\geq 0}$ *is the standard one-dimensional Brownian motion.*

Compare this convergence in law with Theorem A.3 in view of (A.7). We see that $\mathtt{N}_n\,/\mathbb{E}(\,\mathtt{N}_n)$ doesn't converge to 1 with probability one, but converges in law to a non-degenerate random variable. There is a formula for the probability density function ρ of the random variable $\mathcal{F}$, namely

$$\rho(u) = \frac{8}{\sqrt{2\pi}} \sum_{m=1}^{+\infty} (-1)^{m-1} m^2\, \mathrm{e}^{-\frac{m^2u^2}{2}},\, u \in \mathbb{R}_+\,. \tag{A.10}$$

(So the cumulative distribution function of $\mathcal{F}$ is continuous.) This is proved by Feller [4].

We end this section by an important remark.

Remark A.7. *Looking at the proof of Theorem 6.2 in [5], we have that* $\mathbb{E}(\mathtt{N}_n/\sqrt{n}) \xrightarrow[n\to+\infty]{} \mathbb{E}(\mathcal{F}) = \sqrt{8/\pi}$ *and* $\mathrm{Var}(\mathtt{N}_n/\sqrt{n}) \xrightarrow[n\to+\infty]{} \mathrm{Var}(\mathcal{F}) = 4(\log 2 - 2/\pi)$. *This follows from a uniform bound in* n *of the third moment of* $\mathtt{N}_n/\sqrt{n}$*, which implies that the square of* $\mathtt{N}_n/\sqrt{n}$ *is uniformly integrable. This is a well-known sufficient condition to ensure, from the convergence in law, the convergence of the first two moments of* $\mathtt{N}_n/\sqrt{n}$ *toward the first two moments of* $\mathcal{F}$*. Another way to proceed is to compute directly the first and second moments of* $\mathcal{F}$ *using its density, and to see that the results match with* (A.7) *and* (A.8)*. Note also that, by classical properties of the Brownian motion, one has* $\mathbb{E}(\mathcal{F}) = 2\mathbb{E}(|\mathcal{B}_1^{(1)}|) = 2\sqrt{2/\pi}$ *(twice the expected value of the standard half-normal distribution).*

A.3.2 Case $d = 2$

We first recall the classical approximation [2]:

$$\mathbb{E}(\mathtt{N}_n) = \frac{\pi n}{\log n}\left(1 + \mathcal{O}\left(\frac{\log\log n}{\log n}\right)\right). \tag{A.11}$$

In fact, in order to obtain precise enough approximation of the number of prey consumed (see Section B.2 below) we need an approximation at order 2 for $\mathbb{E}(\mathtt{N}_n)$ that we couldn't find in the literature, so we provide a proof.

Proposition A.8. *For all* $n \geq 2$*, we have*

$$\mathbb{E}(\mathtt{N}_n) = \frac{\pi n}{\log n}\left(1 - \frac{\gamma}{\log n} + \mathcal{O}\left(\frac{1}{(\log n)^2}\right)\right) \tag{A.12}$$

where γ *is the Euler-Mascheroni constant* ($\gamma = -\int_0^\infty \log(u)\,\mathrm{e}^{-u}\,\mathrm{d}u \approx 0,577$).[2]

Proof. We use [6, Theorem 1.3] which gives for any $k \in 2\mathbb{N}$

$$\mathbb{P}(T_0 = k) = \frac{\pi}{k(\log k)^2}\left(1 - \frac{2\gamma}{\log k} + \mathcal{O}\left(\frac{1}{(\log k)^2}\right)\right). \tag{A.13}$$

Hence for all $j \geq 2$ we have

$$\mathbb{P}(T_0 > j) = \sum_{k=j+1}^{+\infty} \mathbb{P}(T_0 = k) = \frac{\pi}{\log j}\left(1 - \frac{\gamma}{\log j} + \mathcal{O}\left(\frac{1}{(\log j)^2}\right)\right)$$

where we approximate in the standard way the series by an integral. Using (A.6) yields (A.12) after some standard but tedious calculations. More precisely, we need an asymptotic expansion for, *e.g.*,

$$\sum_{j=2}^{n} \frac{1}{\log j}$$

(which goes to $+\infty$ when $n \to +\infty$.) The basic idea is to approximate this sum by an integral, and then integrate by parts. Then one can use the following expansion for the offset logarithmic integral:

$$\mathrm{Li}(x) := \int_2^x \frac{\mathrm{d}u}{\log u} = \frac{x}{\log x} + \frac{1!\,x}{(\log x)^2} + \cdots + \frac{(k-1)!\,x}{(\log x)^k} + \mathcal{O}\left(\frac{x}{(\log x)^{k+1}}\right).$$

[2] Note that log stands for the natural logarithm.

We refer to [7, Section 3.3] for a nice exposition. □

Concerning the variance, Jain and Pruitt [5] proved that

$$\mathrm{Var}(\mathtt{N}_n) \underset{n\to+\infty}{\sim} \frac{2\pi^2 K\, n^2}{(\log n)^4} \tag{A.14}$$

where

$$K = -\int_0^1 \frac{\log u}{1-u+u^2}\,\mathrm{d}u + \frac{1}{2} - \frac{\pi^2}{12} \approx 0.8495. \tag{A.15}$$

Finally, Le Gall [8] proved the following result. We introduce the short-hand notation

$$Z_n := \frac{(\log n)^2}{n}\big(\mathtt{N}_n - \mathbb{E}(\mathtt{N}_n)\big). \tag{A.16}$$

Theorem A.9. *We have*

$$Z_n \xrightarrow{\text{law}} -2\pi^2 \mathcal{L}_{\mathcal{G}} \tag{A.17}$$

where the random variable $\mathcal{L}_{\mathcal{G}}$ is the "renormalized self-intersection local time" for planar Brownian motion.

Formally,

$$\mathcal{L}_{\mathcal{G}} = \iint\limits_{\{0\le s<t\le 1\}} \delta_{(0)}(\mathcal{B}_s^{(2)} - \mathcal{B}_t^{(2)})\,\mathrm{d}s\,\mathrm{d}t - \mathbb{E}\left(\iint\limits_{\{0\le s<t\le 1\}} \delta_{(0)}(\mathcal{B}_s^{(2)} - \mathcal{B}_t^{(2)})\,\mathrm{d}s\,\mathrm{d}t \right)$$

where $(\mathcal{B}_t^{(2)})_{t\ge 0}$ is a two-dimensional (standard) Brownian motion. Also formally $\mathbb{E}(\mathcal{L}_{\mathcal{G}}) = 0$, as it should be since it is the limit of centered random variables. Notice the unusual normalization by $n/(\log n)^2$, and the fact that the limiting random variable is not Gaussian. An elementary rigorous construction of $\mathcal{L}_{\mathcal{G}}$ is provided in [9].

The following uniform control of the exponential moment of the random variables Z_n will be essential below. See [10] (Theorem 5.4 p. 26) for a proof.

Theorem A.10. *There exists $\theta > 0$ such that*

$$\sup_{n\in\mathbb{N}} \mathbb{E}\left(\exp\left(\theta|Z_n|\right)\right) < +\infty. \tag{A.18}$$

By standard arguments, we deduce the following corollaries.

Corollary A.1. *There exist $c_1, c_2 > 0$ such that*

$$\sup_{n\in\mathbb{N}} \mathbb{P}\big(|Z_n| > u\big) \le c_1\,\mathrm{e}^{-c_2 u},\ u > 0. \tag{A.19}$$

Proof. By Markov inequality we have (since $\theta > 0$)

$$\mathbb{P}\big(|Z_n| > u\big) = \mathbb{P}\big(\theta|Z_n| > \theta u\big) = \mathbb{P}\Big(\mathrm{e}^{\theta|Z_n|} > \mathrm{e}^{\theta u}\Big) \le \mathbb{E}\left(\exp\left(\theta|Z_n|\right)\right)\mathrm{e}^{-\theta u}.$$

This proves (A.19) with $c_1 = \sup_{n\in\mathbb{N}} \mathbb{E}\left(\exp\left(\theta|Z_n|\right)\right)$ and $c_2 = \theta$. □

Corollary A.2. *We have*

$$\lim_{n\to+\infty} \mathbb{E}\big(Z_n^2\big) = \mathbb{E}\big((-2\pi^2\mathcal{L}_{\mathcal{G}})^2\big) = \mathrm{Var}(2\pi^2\mathcal{L}_{\mathcal{G}}) = 2\pi^2 K \tag{A.20}$$

where K is defined in (A.15).

Proof. A classical condition implying that convergence in law of Z_n to $-2\pi^2\mathcal{L}_{\mathcal{G}}$ enforces convergence of $\mathbb{E}(Z_n^2)$ to $\mathbb{E}\big((-2\pi^2\mathcal{L}_{\mathcal{G}})^2\big)$ is uniform integrability of $\big(Z_n^2\big)_{n\in\mathbb{N}}$ (see Theorem 3.5 p. 31 in [11]). Using Corollary A.1, it is straightfoward to obtain $\sup_{n\in\mathbb{N}} \mathbb{E}\big(Z_n^3\big) < +\infty$, which implies the desired uniform integrability. □

Remark A.11. *Notice that the previous proof actually shows that, for all $p \geq 1$, $\mathbb{E}(|Z_n|^p)$ converges to the p-th moment of $-2\pi^2\mathcal{L}_{\mathcal{G}}$.*

A.3.3 Case $d = 3$

Dvoretsky and Erdös [2] proved that

$$\mathbb{E}(\mathtt{N}_n) = \kappa(3)\, n + \mathcal{O}\big(\sqrt{n}\,\big), \tag{A.21}$$

where $\kappa(3) \approx 0.6595$ (recall that this is the probability that the walk never returns to the origin). This is consistent with (A.2). Jain and Pruitt [12] (see Theorems 2 and 4) proved the following results.

Theorem A.12. *We have*

$$\frac{\mathtt{N}_n - \kappa(3)n}{\sigma\sqrt{n\log n}} \xrightarrow{\text{law}} \mathcal{N}(0,1) \tag{A.22}$$

where $\mathcal{N}(0,1)$ is a standard Gaussian random variable (mean 0 and variance 1), and

$$\sigma = \frac{3\sqrt{3}\,\kappa(3)^2}{\sqrt{2}\pi}. \tag{A.23}$$

We also have

$$\mathrm{Var}(\,\mathtt{N}_n) \underset{n\to+\infty}{\sim} \sigma^2\, n\log n.$$

A.4 More general random walks

For the sake of simplicity, we considered only the simplest random walks, namely, simple symmetric random walks. In fact, all the previous results hold true for a much more general class of random walks, up to minor changes, that we briefly describe. We refer to the book of [13] for more informations on random walks. We consider increments ξ_k's ($k \geq 1$) that are independent and identically distributed random variables taking values in $\mathbb{Z}^d$, not necessarily in $\{\pm\,\mathrm{e}^{(1)}, \ldots, \pm\,\mathrm{e}^{(d)}\}$. (The case treated so far is the very special case when, if the walk is at a given site, the next move is to choose one of the $2d$ nearest neighbors of that site with probability $(2d)^{-1}$.) The corresponding random walk is defined by $X_0 = 0$ (so we suppose that the walk starts at the origin of $\mathbb{Z}^d$), and $X_n = \sum_{k=1}^n \xi_k$, $n = 1, 2, \ldots$. We assume that $\mathbb{E}(\xi_1) = 0$ and $\mathbb{E}(|\xi_1|^2) < +\infty$.[3]

[3] For $i \in \mathbb{Z}^d$, $|i|^2 := (i^{(1)})^2 + \cdots + (i^{(d)})^2$.

An important subclass of random walks with these two properties is the class of finite-range symmetric random walks. This means that there exists a finite set $V = \{i_1, \dots, i_r\} \subset \mathbb{Z}^d \backslash \{0\}$ which is generating (that is, every $j \in \mathbb{Z}^d$ can be written as $\alpha_1 i_1 + \cdots + \alpha_r i_r$ for some $\alpha_1, \dots, \alpha_r \in \mathbb{Z}$, so that the walk will be irreducible, and a function $\varrho : V \to]0, 1]$ with $\varrho(i_1) + \cdots + \varrho(x_r) = 1$, defining a symmetric probability distribution p on $\mathbb{Z}^d$ as follows: $p(i_k) = p(-i_k) = \frac{1}{2}\varrho(i_k)$ $(i_k \in V)$. (Notice that we consider only the case $p(0) = 0$, that is, the walk has to leave the site where it is with probability one.) Given p, one can define $(X_n)_{n\geq 0}$ as the (time-homogeneous) Markov chain with state space $\mathbb{Z}^d$ and transition probabilities $\mathbb{P}(X_{n+1} = \ell | X_n = k) = p(\ell - k)$, or as $X_n = \sum_{k=1}^n \xi_k$ where the ξ_k's are independent random variables with distribution p. The simple symmetric random walk is the case where $V = \{\mathrm{e}^{(1)}, \dots, \mathrm{e}^{(d)}\}$.

We now indicate how the results of Section A.3 generalize.

We denote by $Q = \big(\mathbb{E}(\xi_1^{(i)} \xi_1^{(j)})\big)_{1\leq i,j\leq d}$ the covariance matrix, and we let $\sigma^2 := \big(\det Q\big)^{1/d}$.

Theorem A.2 remains true for the class of random walks described above. In fact, having integrable increments is enough, see [1, p. 38].

Theorem A.3 can be generalized in dimension $d = 2$ for any random walk as above, provided it is recurrent, see Theorem 3.1 in [5].

Concerning Section A.3.1 ($d = 1$), Theorem A.6 is true for any random walk as defined above, up to replacing the interval $0 \leq s \leq 1$ by $0 \leq s \leq \sigma^2$.

Concerning the results listed in Section A.3.2 ($d = 2$), one has $\lim_{n\to+\infty}(\log n/n)\ \mathtt{N}_n = 2\pi\sigma^2$ almost-surely. Approximation (A.12) relies on (A.13) which remains the same, up to a multiplicative constant:

$$\mathbb{P}(T_0 = k) = \frac{2\pi\sigma^2}{k(\log k)^2}\left(1 - \frac{2\gamma}{\log k} + \mathcal{O}\left(\frac{1}{(\log k)^2}\right)\right).$$

This is because we can use [6, Theorem 1.3].

Theorem A.9 remains true with $-2\pi^2\mathcal{L}_{\mathcal{G}}$ replaced by $-4\pi^2\sigma^2\,\mathcal{L}_{\mathcal{G}}$, see [8]. Regarding the variance, (A.14) remains the same, up to the constant (see [5], Theorem 4.2): $\mathrm{Var}(\mathtt{N}_n) \underset{n\to+\infty}{\sim} \frac{c\,n^2}{(\log n)^4}$ where $c = 8\pi^2\,K\,\sigma^4$ (where K is defined in (A.15)).

Concerning Section A.3.3 ($d = 3$), we get the same behavior for the above class of random walks, up to constants that depend on ξ_1, see [14].

Remark A.13 (Random walks with a drift). *The situation is very different when $\mathbb{E}(\xi_1) \neq 0$ (non-zero drift). In that case, the walk is strongly transient regardless of the dimension. We recall that a random walk is either transient or recurrent. Transience means that the probability that the walk never comes back to the origin is strictly positive, that is, $\kappa(d) > 0$ (see (A.1)). There are recurrent random walks only if the dimension is one or two. The simple symmetric random walk in dimensions 1 and 2 is recurrent. We will not define strong transience here. For instance, every random walk such that $\mathbb{E}(\xi_1) \neq 0$ and $\mathbb{E}(|\xi_1|^2) < +\infty$ is strongly transient. We just want to emphasize that, in that case, discarding the trivial case where the range grows deterministically (which is when $\kappa(d) = 1$), its variance grows like a constant times n, and a*

central limit theorem in the classical form is true: there exists $\sigma^2 > 0$ *such that* $(\mathtt{N}_n - n\kappa(d))/(\sigma\sqrt{n}) \xrightarrow{\text{law}} N(0,1)$*, see [14] for details.*

Remark A.14. *Notice that the random walk may take place on a proper subgroup of* $\mathbb{Z}^d$*. In this case, the subgroup is isomorphic to some* $\mathbb{Z}^{d'}$ *for* $d' \leq d$*. If* $d' < d$*, then the transformation should be made and the problem considered in* d' *dimensions. We implicitly assumed that this reduction had been made, if necessary, and that* d *is the genuine dimension of the random walk. (This means in particular that the determinant of the covariance matrix of the random walk is not equal to* 0*.)*

B The number of consumed prey

All proofs and results given in this section are new.

B.1 Process dual to the range

Observing that $(\mathtt{N}_n)_{n\geq 1}$ is an increasing process, it is natural to define its "inverse", namely

$$S_k = \inf\{n \geq k : \mathtt{N}_n \geq k\},\ k \geq 1. \tag{B.1}$$

This is the smallest number of steps for the walk to visit at least k distinct sites. We have the following fundamental "duality relation"

$$\{\mathtt{N}_n \leq k\} = \{n \leq S_k\}. \tag{B.2}$$

In particular, studying the law of $\mathtt{N}_n$ is equivalent to studying the law of S_k. Observe that, for each k, S_k is a stopping time.

B.2 Connecting the number of consumed prey to the range of the random walk

We define two important parameters:

- τ_e, defined as the time needed for a predator to go across an edge of the lattice $\mathbb{Z}^d$
- τ_h, defined as the handling time, *i.e.*, the time taken by the predator to consume one prey.

The dimensionless parameter τ_h/τ_e will show up in many instances. We will always assume that $\tau_e > 0$ (τ_h can be equal to 0). The first one gives a time scale with respect to which we can say what a large time t means. Then, we define the stochastic process giving the evolution of our system. It is the joint process made of the random walk $(X_k)_{k\geq 0}$ and the corresponding sequence of (random) times $(T_k)_{k\geq 0}$ at which the walk (the predator) visits the sites.

Let $(X_k, T_k)_{k\geq 0}$ be the double sequence of random variables giving the sites that the predator visits (that is, the position of the random walk), together with the corresponding arrival times. The random walk $(X_k)_{k\geq 0}$ we consider is the simple symmetric random walk defined in the previous section (recall that $X_0 = (0, \dots, 0)$). We can recursively define the arrival times by setting $T_0 = 0$, and letting

$$T_{k+1} = \begin{cases} T_k + \tau_h + \tau_e & \text{if} \quad X_k \notin \{X_0, X_1, \dots X_{k-1}\} \\ T_k + \tau_e & \text{otherwise.} \end{cases}$$

The condition $X_k \notin \{X_0, X_1, \dots X_{k-1}\}$ is equivalent to $\mathtt{N}_k > \mathtt{N}_{k-1}$. Then, the number of prey found before time t is

$$R_t = \mathrm{Card}\big\{k \geq 0 : T_k \leq t,\, \mathtt{N}_k > \mathtt{N}_{k-1}\big\} = \mathrm{Card}\big\{k \geq 0 : T_k \leq t, X_k \notin \{X_1, \dots X_{k-1}\}\big\}.$$

The functional response (the consumption rate) is then defined as

$$F_t = \frac{R_t}{t}.$$

Now, by definition of R_t and using (B.2), we have

$$\{R_t > k\} = \{S_k \tau_e + (k-1)\,\tau_h < t\} = \left\{S_k < \frac{t}{\tau_e} - (k-1)\frac{\tau_h}{\tau_e}\right\} = \big\{\mathtt{N}_{n(t)} > k\big\} \tag{B.3}$$

where

$$n(t) := n_k(t) = \left\lfloor \frac{t}{\tau_e} - (k-1)\frac{\tau_h}{\tau_e} \right\rfloor \tag{B.4}$$

where $\lfloor \cdot \rfloor$ denotes integer part. (For $n(t)$ to be larger than or equal to 1, there is an obvious constraint on t and k, namely $\frac{t}{\tau_e} \geq (k-1)\frac{\tau_h}{\tau_e} + 1$.)

B.2.1 Case $d = 1$

We have the following result.

Theorem B.1. *As $t \to +\infty$, we have*

$$\frac{R_t}{\sqrt{t/\tau_e}} \xrightarrow{\text{law}} \max_{0\leq s\leq 1} \mathcal{B}_s^{(1)} - \min_{0\leq s\leq 1} \mathcal{B}_s^{(1)} \tag{B.5}$$

where $(\mathcal{B}_s^{(1)})_{s\geq 0}$ is the standard one-dimensional Brownian motion.

Observe that τ_h plays no role in the limiting random variable.

Proof. Let $t > 0$. For convenience, we set $t_e := t/\tau_e$ (dimensionless parameter counting time in units of τ_e). Let $u \in \mathbb{R}$. Using (B.3) and (B.4), we have

$$\mathbb{P}\left(\frac{R_t}{\sqrt{t_e}} \leq u\right) = \mathbb{P}\left(\sqrt{\frac{n(t)}{t_e}}\,\frac{\mathtt{N}_{n(t)}}{\sqrt{n(t)}} \leq u\right) \tag{B.6}$$

where

$$n(t) = \left\lfloor t_e - \left(u\sqrt{t_e} - 1\right)\frac{\tau_h}{\tau_e} \right\rfloor .$$

Since $\sqrt{\frac{n(t)}{t_e}} \to 1$ as $t \to +\infty$, using Slutsky's theorem and Theorem A.6, we obtain

$$\sqrt{\frac{n(t)}{t_e}}\,\frac{\mathtt{N}_{n(t)}}{\sqrt{n(t)}} \xrightarrow{\text{law}} \mathcal{F}$$

where $\mathcal{F} = \max_{0\le s\le 1}\mathcal{B}_s^{(1)} - \min_{0\le s\le 1}\mathcal{B}_s^{(1)}$. This means that the right-hand side in (B.6) goes to $\mathbb{P}(\mathcal{F} \le u)$ (its cumulative distribution function is continuous since $\mathcal{F}$ has a density). [4] But, since $u \in \mathbb{R}$ is arbitrary, we obtain that the left-hand side in (B.6) goes to $\mathbb{P}(\mathcal{F} \le u)$ for all $u \in \mathbb{R}$, which entails the convergence in law of $R_t/\sqrt{t_e}$ to $\mathcal{F}$. □

The first two moments of $R_t/\sqrt{t/\tau_e}$ do converge to those of $\max_{0\le s\le 1}\mathcal{B}_s^{(1)} - \min_{0\le s\le 1}\mathcal{B}_s^{(1)}$.

Proposition B.2. *We have*

$$\mathbb{E}\left(\frac{R_t}{\sqrt{t/\tau_e}}\right) \xrightarrow[t\to+\infty]{} \mathbb{E}\left(\max_{0\le s\le 1}\mathcal{B}_s^{(1)} - \min_{0\le s\le 1}\mathcal{B}_s^{(1)}\right) = 2\sqrt{\frac{2}{\pi}} \approx 1.5958,$$

and

$$\mathrm{Var}\left(\frac{R_t}{\sqrt{t/\tau_e}}\right) \xrightarrow[t\to+\infty]{} \mathrm{Var}\left(\max_{0\le s\le 1}\mathcal{B}_s^{(1)} - \min_{0\le s\le 1}\mathcal{B}_s^{(1)}\right) = 4\left(\log 2 - \frac{2}{\pi}\right) \approx 0.2261.$$

Proof. In view of Remark A.7, we show how to control the third moment of $\widetilde{R}_t := R_t/\sqrt{t_e}$ (where $t_e = t/\tau_e$), uniformly in t. Since $\widetilde{R}_t$ is a positive random variable, we only need to control the tail probability $\mathbb{P}\big(\widetilde{R}_t > u\big)$ for $u > 0$. Taking $n(t) = \left\lfloor t_e - (k-1)\frac{\tau_h}{\tau_e}\right\rfloor$ with $k = k(t,u) = u\sqrt{t_e}$, we get at once using (B.3) and the obvious inequality $\mathtt{N}_{n(t)} \le \mathtt{N}_{\lfloor t_e\rfloor}$ that

$$\mathbb{P}\big(\widetilde{R}_t > u\big) = \mathbb{P}\big(R_t > k\big) \le \mathbb{P}\big(\mathtt{N}_{\lfloor t_e\rfloor} > k\big) = \mathbb{P}\left(\frac{\mathtt{N}_{\lfloor t_e\rfloor}}{\sqrt{t_e}} > u\right).$$

We conclude by using Theorem 6.2 in [5] which states that $\mathbb{E}\left[\left(\frac{\mathtt{N}_{\lfloor t_e\rfloor}}{\sqrt{t_e}}\right)^3\right] = \mathcal{O}(1)$, and the formula $\mathbb{E}\big(\widetilde{R}_t^3\big) = 2\int_0^{+\infty} u^2\mathbb{P}\big(\widetilde{R}_t > u\big)\,\mathrm{d}u$. □

B.2.2 Case $d = 2$

The situation for $d = 2$ is completely different from that in dimension $d = 1$.

Theorem B.3. *We have*

$$\frac{\left(\log\left(\frac{t}{\tau_e}\right)\right)^2}{\frac{t}{\tau_e}}\left(R_t - \frac{\pi\,\frac{t}{\tau_e}}{\log\left(\frac{t}{\tau_e}\right)}\right) \xrightarrow{\text{law}} -\pi\left(2\pi\mathcal{L}_{\mathcal{G}} + \frac{\pi\,\tau_h}{\tau_e} + \gamma\right), \text{ as } t \to +\infty \tag{B.7}$$

where $\mathcal{L}_{\mathcal{G}}$ is the random variable appearing in Theorem A.9.

[4] Recall that if $(Y_n)_{n\ge 0}$ is a sequence of real-valued random variables, and Y a real-valued random variable, then $Y_n \xrightarrow{\text{law}} Y$ if and only if $\mathbb{P}(Y_n \le u) \to \mathbb{P}(Y \le u)$, as $n \to +\infty$, at every point where $u \mapsto \mathbb{P}(Y \le u)$ is continuous.

Proof. Let $t > 0$. As before, we set $t_e := t/\tau_e$. To alleviate notation, let $a(t) := (\log t)^2/t$, and

$$\widetilde{R}_t := a(t_e)\left(R_t - \frac{\pi t_e}{\log t_e}\right).$$

Using (A.12), we rewrite the left-hand side of (B.7):

$$\widetilde{R}_t = a(t_e)\left(R_t - \mathbb{E}\left(\mathtt{N}_{\lfloor t_e \rfloor}\right)\right) - \pi\gamma + \mathcal{O}\left(\frac{1}{\log t_e}\right). \tag{B.8}$$

Hence, by Slutsky's theorem, if $a(t_e)\left(R_t - \mathbb{E}\left(\mathtt{N}_{\lfloor t_e \rfloor}\right)\right)$ converges in law to a random variable, say, $\mathcal{W}$, then $\widetilde{R}_t$ converges in law to

$$\mathcal{W} - \pi\gamma. \tag{B.9}$$

We now want to use (B.3), that is

$$\{R_t \le k\} = \{\mathtt{N}_{n(t)} \le k\}, \tag{B.10}$$

where we take

$$n(t) = n(t,u) = \left\lfloor t_e - (k-1)\frac{\tau_h}{\tau_e}\right\rfloor \quad \text{and} \quad k = k(t,u) := \left\lfloor a(t_e)^{-1}u + \mathbb{E}\left(\mathtt{N}_{\lfloor t_e \rfloor}\right)\right\rfloor,$$

and where $u \in \mathbb{R}$ is a continuity point of the cumulative distribution function of $-2\pi^2\mathcal{L}_{\mathcal{G}}$. Hence, the equality between the events in (B.10) writes

$$\left\{a(t_e)\left(R_t - \mathbb{E}\left(\mathtt{N}_{\lfloor t_e \rfloor}\right)\right) \le u\right\} = \left\{a(t_e)\left(\mathtt{N}_{n(t)} - \mathbb{E}\left(\mathtt{N}_{\lfloor t_e \rfloor}\right)\right) \le u\right\}. \tag{B.11}$$

Using Theorem A.9, with n replaced by $n(t)$, we have

$$a(n(t))\left(\mathtt{N}_{n(t)} - \mathbb{E}(\mathtt{N}_{n(t)})\right) \xrightarrow{\text{law}} -2\pi^2\mathcal{L}_{\mathcal{G}}\,. \tag{B.12}$$

(Observe that $n(t) \to +\infty$, as $t \to +\infty$, since $\mathbb{E}\left(\mathtt{N}_{\lfloor t_e \rfloor}\right) \underset{t\to+\infty}{\sim} (\pi t_e)/\log t_e$ by (A.11), whence $n(t) \underset{t\to+\infty}{\sim} t_e$.) To use (B.12), we write

$$a(t_e)\left(\mathtt{N}_{n(t)} - \mathbb{E}\left(\mathtt{N}_{\lfloor t_e \rfloor}\right)\right) = \frac{a(t_e)}{a(n(t))}\left(a(n(t))\left(\mathtt{N}_{n(t)} - \mathbb{E}\left(\mathtt{N}_{n(t)}\right)\right)\right) + a(t_e)\,\mathbb{E}\left(\mathtt{N}_{n(t)} - \mathtt{N}_{\lfloor t_e \rfloor}\right)\Big). \tag{B.13}$$

Using (A.11), and the fact that $k \underset{t\to+\infty}{\sim} \pi\, t_e/\log(t_e)$, we have

$$\mathbb{E}\left(\mathtt{N}_{\lfloor t_e \rfloor}\right) - \mathbb{E}\left(\mathtt{N}_{n(t)}\right) \underset{t\to+\infty}{\sim} \frac{\pi}{\log t_e}\frac{\tau_h k}{\tau_e} \underset{t\to+\infty}{\sim} \frac{\tau_h t}{\tau_e^2}\frac{\pi^2}{(\log t_e)^2}.$$

Hence

$$a(t_e)\,\mathbb{E}\left(\mathtt{N}_{n(t)} - \mathtt{N}_{\lfloor t_e \rfloor}\right) \underset{t\to+\infty}{\sim} -\pi^2\frac{\tau_h}{\tau_e}. \tag{B.14}$$

We leave to the reader check that $a(n(t))/a(t_e) \underset{t\to+\infty}{\sim} 1$. Then, we apply Slutsky's theorem once more, together with (B.12), to obtain that the right-hand side of (B.13) converges in law to $-2\pi^2\mathcal{L}_{\mathcal{G}} - (\pi^2\tau_h)/\tau_e$. Hence we obtain by (B.13) that

$$a(t_e)\left(\mathtt{N}_{n(t)} - \mathbb{E}\left(\mathtt{N}_{\lfloor t_e \rfloor}\right)\right) \xrightarrow{\text{law}} -2\pi^2\mathcal{L}_{\mathcal{G}} - \pi^2\frac{\tau_h}{\tau_e}.$$

It follows that $\mathbb{P}\big(a(t_e)\left((\mathtt{N}_{n(t)} - \mathbb{E}\left(\mathtt{N}_{\lfloor t_e \rfloor}\right)\right) \leq u\big) \xrightarrow[t\to+\infty]{} \mathbb{P}\big(-2\pi^2\mathcal{L}_{\mathcal{G}} - (\pi^2\tau_h)/\tau_e \leq u\big)$ for any $u \in \mathbb{R}$ is an arbitrary continuity point of the cumulative distribution function. We deduce, using (B.11), that $a(t_e)\big(R_t - \mathbb{E}\left(\mathtt{N}_{\lfloor t_e \rfloor}\right)\big) \xrightarrow{\text{law}} -2\pi^2\mathcal{L}_{\mathcal{G}} - (\pi^2\tau_h)/\tau_e$. Therefore, coming back to (B.8) (see the sentence right after it, and also (B.9)), we finally obtain that $\mathcal{W} = -2\pi^2\mathcal{L}_{\mathcal{G}} - (\pi^2\tau_h)/\tau_e$, which entails that

$$\widetilde{R}_t \xrightarrow{\text{law}} -2\pi^2\mathcal{L}_{\mathcal{G}} - \frac{\pi^2\tau_h}{\tau_e} - \pi\gamma$$

which after rearrangement is exactly (B.7), which ends the proof. □

The following result is the analog of Corollary A.2, and its proof goes along the same lines.

Proposition B.4. *We have*

$$\mathbb{E}(R_t) \underset{t\to+\infty}{\sim} \frac{\pi t_e}{\log t_e} \tag{B.15}$$

and

$$\left(\frac{\left(\log\left(\frac{t}{\tau_e}\right)\right)^2}{\frac{t}{\tau_e}}\right)^2 \mathrm{Var}\left(R_t\right) \xrightarrow[t\to+\infty]{} 2\pi^2 K, \tag{B.16}$$

where K is defined in (A.15).

Proof. As before, we use the notations $t_e = t/\tau_e$, $a(t) = (\log t)^2/t$, and

$$\widetilde{R}_t := a(t_e)\left(R_t - \frac{\pi t_e}{\log t_e}\right).$$

We first show how to control $\mathbb{P}\big(\widetilde{R}_t > u\big)$ for all $u > 0$, uniformly in t (which is the crucial point). We use again (B.3), that is,

$$\{R_t > k\} = \{\mathtt{N}_{n(t)} > k\}, \tag{B.17}$$

where we now take

$$n(t) = n(t,u) = \left\lfloor t_e - (k-1)\frac{\tau_h}{\tau_e}\right\rfloor, \quad k = k(t,u) := \left\lfloor a(t_e)^{-1}u + \frac{\pi t_e}{\log t_e}\right\rfloor.$$

Since $\mathtt{N}_{n(t)} \leq \mathtt{N}_{\lfloor t_e \rfloor}$ we have

$$\mathbb{P}(R_t > k) = \mathbb{P}(\mathtt{N}_{n(t)} > k) \leq \mathbb{P}(\mathtt{N}_{\lfloor t_e \rfloor} > k). \tag{B.18}$$

We now bound the rightmost term:

$$\begin{aligned}\mathbb{P}(\mathtt{N}_{\lfloor t_e \rfloor} > k) &= \mathbb{P}\left(a(t_e)\left(\mathtt{N}_{\lfloor t_e \rfloor} - \frac{\pi t_e}{\log t_e}\right) > u\right) \\ &= \mathbb{P}\left(a(t_e)\left(\mathtt{N}_{\lfloor t_e \rfloor} - \mathbb{E}(\mathtt{N}_{\lfloor t_e \rfloor})\right) > u + a(t_e)\left(\frac{\pi t_e}{\log t_e} - \mathbb{E}(\mathtt{N}_{\lfloor t_e \rfloor})\right)\right).\end{aligned}$$

We use again (A.12) to get

$$a(t_e)\left(\frac{\pi t_e}{\log t_e} - \mathbb{E}(\mathtt{N}_{\lfloor t_e \rfloor})\right) = \pi\gamma + \mathcal{O}\left(\frac{1}{\log t_e}\right),$$

which is larger than $\pi\gamma/2$ for all t larger than some t_0 (independent of u). It follows from (B.18) that

$$\mathbb{P}\big(\widetilde{R}_t > u\big) = \mathbb{P}(R_t > k) \le \mathbb{P}\left(a(t_e)\left(\mathtt{N}_{\lfloor t_e\rfloor} - \mathbb{E}(\mathtt{N}_{\lfloor t_e\rfloor})\right) > u + \frac{\pi\gamma}{2}\right),\ t \ge t_0,$$

therefore, using (A.19), we obtain

$$\sup_{t\ge t_0} \mathbb{P}\big(\widetilde{R}_t > u\big) \le c_1\, \mathrm{e}^{-c_2 u}. \tag{B.19}$$

We now turn to show how to control $\mathbb{P}\big(\widetilde{R}_t < -u\big)$ for all $u > 0$, uniformly in t. We have

$$\mathbb{P}\big(\widetilde{R}_t < -u\big) = \mathbb{P}\left(a(t_e)\left(R_t - \frac{\pi t_e}{\log t_e}\right) < -u\right) = \mathbb{P}\left(R_t < -\frac{u}{a(t_e)} + \frac{\pi t_e}{\log t_e}\right) = \mathbb{P}(\mathtt{N}_{n(t)} < k)$$

where we used (B.3) with $k = k(t,u) := -a(t_e)u + (\pi t_e)/\log t_e$, whence

$$n(t) \ge \left\lfloor t_e + \left(\frac{u}{a(t_e)} - \frac{\pi t_e}{\log t_e}\right)\frac{\tau_h}{\tau_e}\right\rfloor \ge \left\lfloor t_e\left(1 - \frac{\pi\tau_h}{\tau_e}\frac{1}{\log t_e}\right)\right\rfloor =: n'(t).$$

(Observe that the rightmost term does not depend on u.) It follows that $\mathtt{N}_{n(t)} \ge \mathtt{N}_{\lfloor t_e\left(1-\frac{\pi\tau_h}{\tau_e}\frac{1}{\log t_e}\right)\rfloor}$, hence

$$\begin{aligned}
\mathbb{P}\big(\widetilde{R}_t < -u\big) &\le \mathbb{P}\left(\mathtt{N}_{n'(t)} < k\right) \\
&= \mathbb{P}\left(a(t_e)\left(\mathtt{N}_{n'(t)} - \frac{\pi t_e}{\log t_e}\right) < -u\right) \\
&= \mathbb{P}\left(a(t_e)\left(\mathtt{N}_{n'(t)} - \mathbb{E}\left(\mathtt{N}_{n'(t)}\right)\right) < -u + a(t_e)\left(\frac{\pi t_e}{\log t_e} - \mathbb{E}\left(\mathtt{N}_{n'(t)}\right)\right)\right).
\end{aligned}$$

Once more, we use(A.12), and it is left to the reader to check that

$$a(t_e)\left(\frac{\pi t_e}{\log t_e} - \mathbb{E}\left(\mathtt{N}_{n'(t)}\right)\right) = -\pi\left(\pi\frac{\tau_h}{\tau_e} - \gamma\right) + \mathcal{O}\left(\frac{1}{\log t_e}\right).$$

There exists t_0' (independent of u) such that for all $t \ge t_0'$ the right-hand side is less than or equal to $-(\pi^2\tau_h)/\tau_e + (3\pi\gamma)/2$, hence, using (A.19), we obtain

$$\mathbb{P}\big(\widetilde{R}_t < -u\big) \le c_1\, \mathrm{e}^{\frac{3\pi\gamma c_2}{2}}\, \mathrm{e}^{-c_2 u},$$

therefore

$$\sup_{t\ge t_0'} \mathbb{P}\big(\widetilde{R}_t < -u\big) \le c_1\, \mathrm{e}^{\frac{3\pi\gamma c_2}{2}}\, \mathrm{e}^{-c_2 u}. \tag{B.20}$$

Combining (B.19) and (B.20), we thus proved that

$$\sup_{t\ge t_0\vee t_0'} \mathbb{P}\big(|\widetilde{R}_t| > u\big) \le 2c_1\, \mathrm{e}^{\frac{3\pi\gamma c_2}{2}}\, \mathrm{e}^{-c_2 u}.$$

Reasoning as in the proof of Corollary A.2, we deduce that the expected value of the left-hand side of (B.7) converges to the expected value of its right-hand side, that is,

$$a(t_e)\left(\mathbb{E}\big(R_t\big) - \frac{\pi t_e}{\log t_e}\right) \to -\pi\left(\pi\frac{\tau_h}{\tau_e} + \gamma\right),\ \text{as } t \to +\infty. \tag{B.21}$$

(Recall that $\mathbb{E}(\mathcal{L}_{\mathcal{G}}) = 0$.) This implies (B.15). We also know that

$$\mathbb{E}\big(\widetilde{R}_t^2\big) \to \mathbb{E}\left[\left(2\pi^2\mathcal{L}_{\mathcal{G}} + \frac{\pi^2\,\tau_h}{\tau_e} + \pi\gamma\right)^2\right] = \mathrm{Var}(2\pi^2\mathcal{L}_{\mathcal{G}}) + \left(\frac{\pi^2\,\tau_h}{\tau_e} + \pi\gamma\right)^2,\ \text{as } t \to +\infty. \tag{B.22}$$

Since

$$a(t_e)^2 \operatorname{Var}(R_t) = \mathbb{E}\big(\widetilde{R}_t^2\big) - \left(a(t_e)\left(\mathbb{E}\big(R_t\big) - \frac{\pi t_e}{\log t_e}\right)\right)^2 \text{ as } t \to +\infty,$$

(B.16) follows from (B.21) and (B.22). The proof of the proposition is now complete. □

B.2.3 Case $d = 3$

We now deal with the case $d = 3$ which is completely different from the cases $d = 1$ and $d = 2$.

Theorem B.5. *We have*

$$\frac{R_t - \left(\frac{\kappa(3)}{1+\kappa(3)\frac{\tau_h}{\tau_e}}\right)\frac{t}{\tau_e}}{\sqrt{\frac{t}{\tau_e}\log\frac{t}{\tau_e}}} \xrightarrow{\text{law}} \mathcal{N}\big(0,\eta^2\big), \text{ as } t \to +\infty, \tag{B.23}$$

where $\mathcal{N}\big(0,\eta^2\big)$ is a centered Gaussian random variable with variance

$$\eta^2 = \frac{\sigma^2}{\left(1+\kappa(3)\frac{\tau_h}{\tau_e}\right)^3}, \tag{B.24}$$

where σ is given in (A.23).

Observe that, when $\tau_h \to 0$, the coefficient of t/τ_e in (B.23) goes to $\kappa(3)$, and η goes σ. So, in the limit $\tau_h \to 0$, R_t behaves in the same way, in law, as $\mathtt{N}_n$ if n is replaced by t/τ_e (see (A.22).

Proof. Let $t > 0$. Fix $u \in \mathbb{R}$ and recall that $t_e = t/\tau_e$. In view of (B.3) and (B.4) and the normalisation we are interested in for R_t, we choose $k = \lfloor u\,\sigma\sqrt{t_e \log t_e} + c\,t_e \rfloor$, where c is a constant which will be chosen later on, and get

$$\mathbb{P}\left(\frac{R_t - c\,t_e}{\sigma\sqrt{t_e\log t_e}} \le u\right) = \mathbb{P}\left(\frac{\mathtt{N}_{n(t)} - c\,t_e}{\sigma\sqrt{t_e\log t_e}} \le u\right). \tag{B.25}$$

Now we rewrite the random variable that appears in the right-hand side of the previous equation as follows:

$$\frac{\mathtt{N}_{n(t)} - c\,t_e}{\sigma\sqrt{t_e\log t_e}} = \sqrt{\frac{n(t)\log n(t)}{t_e\log t_e}}\,\frac{\mathtt{N}_{n(t)} - \kappa(3)\,n(t)}{\sigma\sqrt{n(t)\log n(t)}} + \frac{1}{\sigma}\,\frac{\kappa(3)\,n(t) - c\,t_e}{\sqrt{t_e\log t_e}}. \tag{B.26}$$

We have

$$\kappa(3)\,n(t) - c\,t_e = \left(\kappa(3)\left(1 - \frac{c\tau_h}{\tau_e}\right) - c\right)t_e - \kappa(3)\,\sigma\frac{\tau_h}{\tau_e}\,u\sqrt{t_e\log t_e} + \mathcal{O}(1).$$

If the coefficient of t_e is not equal to 0, then $(\kappa(3)\,n(t) - c\,t_e)/\sqrt{t_e\log t_e}$ blows up as $t \to +\infty$. To get a finite contribution in the limit, we look for a value of c making this coefficient equal to 0, which works if

$$c = \frac{\kappa(3)}{1+\kappa(3)\frac{\tau_h}{\tau_e}}. \tag{B.27}$$

It is easy to check that

$$n(t) \underset{t\to+\infty}{\sim} \left(1 - \frac{c\,\tau_h}{\tau_e}\right)t_e = \frac{t_e}{1+\kappa(3)\frac{\tau_h}{\tau_e}}.$$

Hence

$$\sqrt{((n(t)\log n(t))/(t_e \log t_e)} \underset{t\to+\infty}{\sim} \frac{1}{\sqrt{1+\kappa(3)\frac{\tau_h}{\tau_e}}}.$$

We now apply Slutsky's theorem, together with Theorem A.12, to get that the right-hand in (B.26) side converges in law to

$$\frac{\mathcal{N}(0,1)}{\sqrt{1+\kappa(3)\frac{\tau_h}{\tau_e}}} - \frac{\kappa(3)\tau_h}{\tau_e}\, u$$

where $\mathcal{N}(0,1)$ is a standard Gaussian random variable. Since the limiting random variable has a density, its cumulative distribution function is continuous, hence we finally obtain (remember (B.26)):

$$\mathbb{P}\left(\frac{\mathtt{N}_{n(t)} - c\, t_e}{\sigma\sqrt{t_e \log t_e}} \le u\right) \xrightarrow[t\to+\infty]{} \mathbb{P}\left(\frac{\mathcal{N}(0,1)}{\sqrt{1+\kappa(3)\frac{\tau_h}{\tau_e}}} - \frac{\kappa(3)\tau_h}{\tau_e}\, u \le u\right) = \mathbb{P}\left(\mathcal{N}' \le u\right)$$

where $\mathcal{N}'$ is a centered Gaussian random variable with variance $1/\big(1+\kappa(3)\frac{\tau_h}{\tau_e}\big)^3$. In view of (B.25), this means that

$$\mathbb{P}\left(\frac{R_t - c\, t_e}{\sigma\sqrt{t_e \log t_e}} \le u\right) \xrightarrow[t\to+\infty]{} \mathbb{P}\left(\mathcal{N}' \le u\right)$$

where c is given in (B.27). Since this is true for an arbitrary $u \in \mathbb{R}$, we thus proved that

$$\frac{R_t - \left(\frac{\kappa(3)}{1+\kappa(3)\frac{\tau_h}{\tau_e}}\right) t_e}{\sqrt{t_e \log t_e}} \xrightarrow{\text{law}} \sigma\, \mathcal{N}'$$

which concludes the proof, since the random variable $\sigma\, G'$ is equal in law to a centered Gaussian random variable with variance $\sigma^2/\big(1+\kappa(3)\frac{\tau_h}{\tau_e}\big)^3$. □

We finish this section by the following proposition.

Proposition B.6. *We have*

$$\mathbb{E}(R_t) \underset{t\to+\infty}{\sim} \left(\frac{\kappa(3)}{1+\kappa(3)\frac{\tau_h}{\tau_e}}\right)\frac{t}{\tau_e} \quad \textit{and} \quad \mathrm{Var}\left(\frac{R_t}{\sqrt{\frac{t}{\tau_e}\log\frac{t}{\tau_e}}}\right) \xrightarrow[t\to+\infty]{} \eta^2,$$

where η is defined in (B.24).

We leave the proof to the reader. It follows the same pattern as before, namely the strategy consists in proving some uniform integrability, which in turn results from the uniform control of the 4th-order moment of $\big(\mathtt{N}_n - \mathbb{E}(\mathtt{N}_n)\big)/\sqrt{n\log n}$ proved in [5](see Theorem 4).

B.3 Coefficients of variation of R_t

Let $\sigma(R_t) := \sqrt{\mathrm{Var}(R_t)}$, that is, $\sigma(R_t)$ is the standard deviation of R_t. We now compute the coefficient of variation defined as $\mathrm{CV}_t^{(d)} = \sigma(R_t)/\mathbb{E}(R_t)$ for $d = 1, 2, 3$.

In dimension one, we deduce from Proposition B.2

$$\mathrm{CV}_t^{(1)} \underset{t\to+\infty}{\sim} \frac{2\sqrt{\log 2 - \frac{2}{\pi}}}{2\sqrt{\frac{2}{\pi}}} \approx 0.3.$$

In dimension two, Proposition B.4 implies that

$$\mathrm{CV}_t^{(d2} \underset{t\to+\infty}{\sim} \frac{\sqrt{2K}}{\log\frac{t}{\tau_e} - \gamma - \pi\frac{\tau_h}{\tau_e}} \approx \frac{1.3}{\log\frac{t}{\tau_e}}.$$

Finally, in dimension 3, Proposition B.6 gives

$$\mathrm{CV}_t^{(3)} \underset{t\to+\infty}{\sim} \frac{3\sqrt{3}\,\kappa(3)}{\sqrt{2}\,\pi\sqrt{1+\kappa(3)\frac{\tau_h}{\tau_e}}}\sqrt{\frac{\log\frac{t}{\tau_e}}{\frac{t}{\tau_e}}} \approx \frac{0.8}{\sqrt{1+0.7\frac{\tau_h}{\tau_e}}}\sqrt{\frac{\log\frac{t}{\tau_e}}{\frac{t}{\tau_e}}}.$$

B.4 Adding prey at random on the lattice

The same approach allows to extend the results on the asymptotic behavior of the functional response to the case where we drop at each site (independently of one another) a prey with probability p. We can follow the same argument as above and now use (B.29) and (B.30) below.

More precisely, we assume that, at each site, we draw a prey at random with probability p, where $p \in (0,1]$ is fixed. The prey are drawn independently of one another. Let us count the number of prey $\mathtt{N}_n^{(p)}$ seen by the predator after n steps, *i.e.*, the number of different sites where there is a prey. Observe that $\mathtt{N}_n^{(1)} = \mathtt{N}_n$. Moreover, the process $\big(\mathtt{N}_n^{(p)}\big)_{n\geq 0}$ can be constructed using $(\mathtt{N}_n)_{n\geq 1}$ as follows. Let $(B_i)_{i\in\mathbb{Z}^d}$ be independent Bernoulli random variables with parameter p. The event $B_i = 1$ corresponds to the presence of a prey at site i. We denote by $Y_k \in \mathbb{Z}^d$ the value of the k-th distinct site visited by the random walk $(X_n)_{n\geq 0}$, so that $(Y_1, \ldots, Y_{\mathtt{N}_n})$ are the sites successively visited after n step. The key observation is that the random variables $V_k = B_{Y_k}$ also form a sequence of independent identically distributed Bernoulli random variables with parameter p, which is independent of $(\mathtt{N}_n)_{n\geq 1}$. Moreover

$$\mathtt{N}_n^{(p)} = \sum_{k=1}^{\mathtt{N}_n} V_k. \tag{B.28}$$

First, we immediately deduce that

$$\mathbb{E}\big(\mathtt{N}_n^{(p)}\big) = p\,\mathbb{E}(\mathtt{N}_n). \tag{B.29}$$

Next, letting $a_n^{(d)} = \mathbb{E}(\mathtt{N}_n)$, recall that $\mathtt{N}_n / a_n^{(d)}$ converges to 1 with probability one in dimensions $d = 2, 3$ (see (A.3), (A.11) and (A.21)). We deduce that

$$\mathbb{P}\left(\frac{\mathtt{N}_n^{(p)}}{a_n^{(d)}} \xrightarrow[n\to+\infty]{} p\right) = 1.$$

Indeed,

$$\frac{\mathtt{N}_n^{(p)}}{a_n^{(d)}} = \frac{\mathtt{N}_n}{a_n^{(d)}}\left(\frac{1}{\mathtt{N}_n}\sum_{k=1}^{\mathtt{N}_n} V_k\right).$$

The term in front of the average goes to 1 with probability one, and the the average goes almost surely to p by the strong law of large numbers applied to the Bernoulli random variables B_k (since $\mathtt{N}_n \to +\infty$ with probability one).

Finally, for the convergence in law, we exploit again the previous results, which can be gathered as :

$$\frac{\mathtt{N}_n - a_n^{(d)}}{b_n^{(d)}} \xrightarrow{\text{law}} \mathcal{W}^{(d)} \tag{B.30}$$

where

$$\begin{aligned}
\mathcal{W}^{(1)} &= \max_{0\le s\le 1} \mathcal{B}_s - \min_{0\le s\le 1} \mathcal{B}_s, \quad a_n^{(1)} = 0, \quad b_n^{(1)} = \sqrt{n}, \\
\mathcal{W}^{(2)} &= -2\pi^2 \mathcal{L}_{\mathcal{G}}, \quad a_n^{(2)} = \frac{\pi n}{\log n}, \quad b_n^{(2)} = \frac{n}{(\log n)^2}, \\
\mathcal{W}^{(3)} &= \mathcal{N}(0,1), \quad a_n^{(3)} = \kappa(3) n, \quad b_n^{(3)} = \sigma\sqrt{n \log n},
\end{aligned}$$

see (A.9), (A.17), and (A.22).

We use Lévy's convergence theorem to get convergence in law for $\mathtt{N}_n^{(p)}$ from the one for $\mathtt{N}_n$. More precisely, (B.28) yields

$$\mathtt{N}_n^{(p)} = p\ \mathtt{N}_n + \sum_{k=1}^{\mathtt{N}_n} (V_k - p).$$

Since $\mathbb{E}\left(\mathrm{e}^{\lambda(V_k - p)}\right) = (1-p)\,\mathrm{e}^{-\lambda p} + p\,\mathrm{e}^{\lambda(1-p)}$ ($\lambda \in \mathbb{C}$), and conditioning upon $\mathtt{N}_n$, we get

$$\begin{aligned}
\mathbb{E}\left(\mathrm{e}^{\mathrm{i}t(\mathtt{N}_n^{(p)} - p a_n^{(d)})/b_n^{(d)}}\right) &= \mathrm{e}^{-\mathrm{i}tpa_n^{(d)}/b_n^{(d)}}\ \mathbb{E}\left(\left((1-p)\,\mathrm{e}^{-\mathrm{i}tp/b_n^{(d)}} + p\,\mathrm{e}^{\mathrm{i}t(1-p)/b_n^{(d)}}\right)^{\mathtt{N}_n} \mathrm{e}^{\mathrm{i}tp\ \mathtt{N}_n\ /b_n^{(d)}}\right) \\
&= \mathrm{e}^{-\mathrm{i}tpa_n^{(d)}/b_n^{(d)}}\ \mathbb{E}\left(\mathrm{e}^{\left(\mathrm{i}tp/b_n^{(d)} + o(1)\right)\ \mathtt{N}_n}\right) \\
&= \mathbb{E}\left(\mathrm{e}^{\mathrm{i}tp(\mathtt{N}_n - a_n^{(d)})/b_n^{(d)}}\right) + o(1) \\
&\xrightarrow[n\to+\infty]{} \mathbb{E}\left(\mathrm{e}^{\mathrm{i}tp\mathcal{W}^{(d)}}\right)
\end{aligned}$$

using (B.30). By Lévy's convergence theorem, this gives

$$\frac{\mathtt{N}_n^{(p)} - p\,a_n^{(d)}}{b_n^{(d)}} \xrightarrow{\text{law}} p\,\mathcal{W}^{(d)}\,.$$

2

C Derivation of the coefficient of variation

C.1 Reminder: Distribution of the consumption rate

The distribution of the number of prey consumed by a single predator after a time t is given in App. B. Recall that the consumption rate (or functional response) after a time t is defined as

$$F_t^{(d)} := \frac{R_t^{(d)}}{t}$$

which gives

$$F_t^{(d)} = \begin{cases} \frac{p}{\sqrt{\tau_e t}}\,\mathcal{W}_t^{(1)} + o_{\mathbb{P}}\left(\frac{1}{\sqrt{t}}\right) & \text{if } d=1 \\ \frac{\pi p}{\tau_e \ln t/\tau_e}\left(1 - \frac{1}{\ln t/\tau_e}\left(\gamma + \pi\frac{\tau_h}{\tau_e} + 2\pi\,\mathcal{W}_t^{(2)}\right)\right) + o_{\mathbb{P}}\left((\frac{1}{\ln t})^2\right) & \text{if } d=2 \\ \frac{\kappa p}{\tau_e+\kappa\tau_h} + p\sqrt{\frac{\ln t/\tau_e}{t\tau_e(1+\kappa\tau_h/\tau_e)^3}}\,\mathcal{W}_t^{(3)} + o_{\mathbb{P}}\left(\sqrt{\frac{\ln t}{t}}\right) & \text{if } d=3 \end{cases} \tag{C.1}$$

where p is the probability that a site contains a prey, $\gamma \approx 0.577$ is Euler-Mascheroni constant, $\kappa \approx 0.659$ is the probability that a simple symmetric random walk never returns to the origin in $\mathbb{Z}^3$, and $\mathcal{W}_t^{(d)} =_{\text{law}} \mathcal{W}^{(d)}$ are different random variables depending on dimensionality (see App. B.2 for details): $\mathcal{W}^{(1)}$ is the difference between the max and min position of a 1-dimensional Brownian motion: $\mathcal{W}^{(1)} = \max_{s\le 1}\mathcal{B}_s^{(1)} - \min_{s\le 1}\mathcal{B}_s^{(1)}$; $W^{(2)} = \mathcal{L}_{\mathcal{G}}$ is the local time of self-intersection of a 2-dimensional Brownian motion; $\mathcal{W}^{(3)} = \mathcal{N}(0,\eta^2)$ is a centred Gaussian distribution with a constant variance η^2. Finally, $o_{\mathbb{P}}(\eta_t)$ is defined such that for any $\varepsilon > 0$, $\mathbb{P}(o_{\mathbb{P}}(\eta_t) \ge \varepsilon\eta_t) \to 0$ as $t \to \infty$.

The mean, variance and the coefficient of variation of the consumption rate F_t are summarized and illustrated in the following table and figures:

Table 1: Summary of statistics for the distribution of the consumption rate.

Dimension	$\mathbb{E}$xpectation	Varariance	Coefficient of variation
1D	$2p\sqrt{\frac{2}{\pi}}\frac{1}{\sqrt{\tau_e t}}$	$4p^2\frac{\ln 2 - 2/\pi}{t\tau_e}$	$\sqrt{\frac{\pi}{2}\ln 2 - 1} \approx 0.298$
2D	$p\frac{\pi/\tau_e}{\ln t/\tau_e}\left(1 - \frac{\gamma+\tau_h\pi/\tau_e}{\ln t/\tau_e}\right)$	$p^2\frac{2K\pi^2}{\tau_e^2(\ln t/\tau_e)^4}$	$\frac{\sqrt{2K}}{\log\frac{t}{\tau_e} - \gamma - \pi\frac{\tau_h}{\tau_e}} \approx \frac{1.3}{\log t/\tau_e}$
3D	$p\frac{\kappa(3)}{\tau_e+\kappa(3)\tau_h}$	$p^2\frac{27\kappa(3)^4}{2\pi^2}\frac{\ln t/\tau_e}{t\tau_e(1+\kappa(3)\tau_h/\tau_e)^3}$	$\frac{0.8}{\sqrt{1+0.7\frac{\tau_h}{\tau_e}}}\sqrt{\frac{\log\frac{t}{\tau_e}}{\frac{t}{\tau_e}}}$

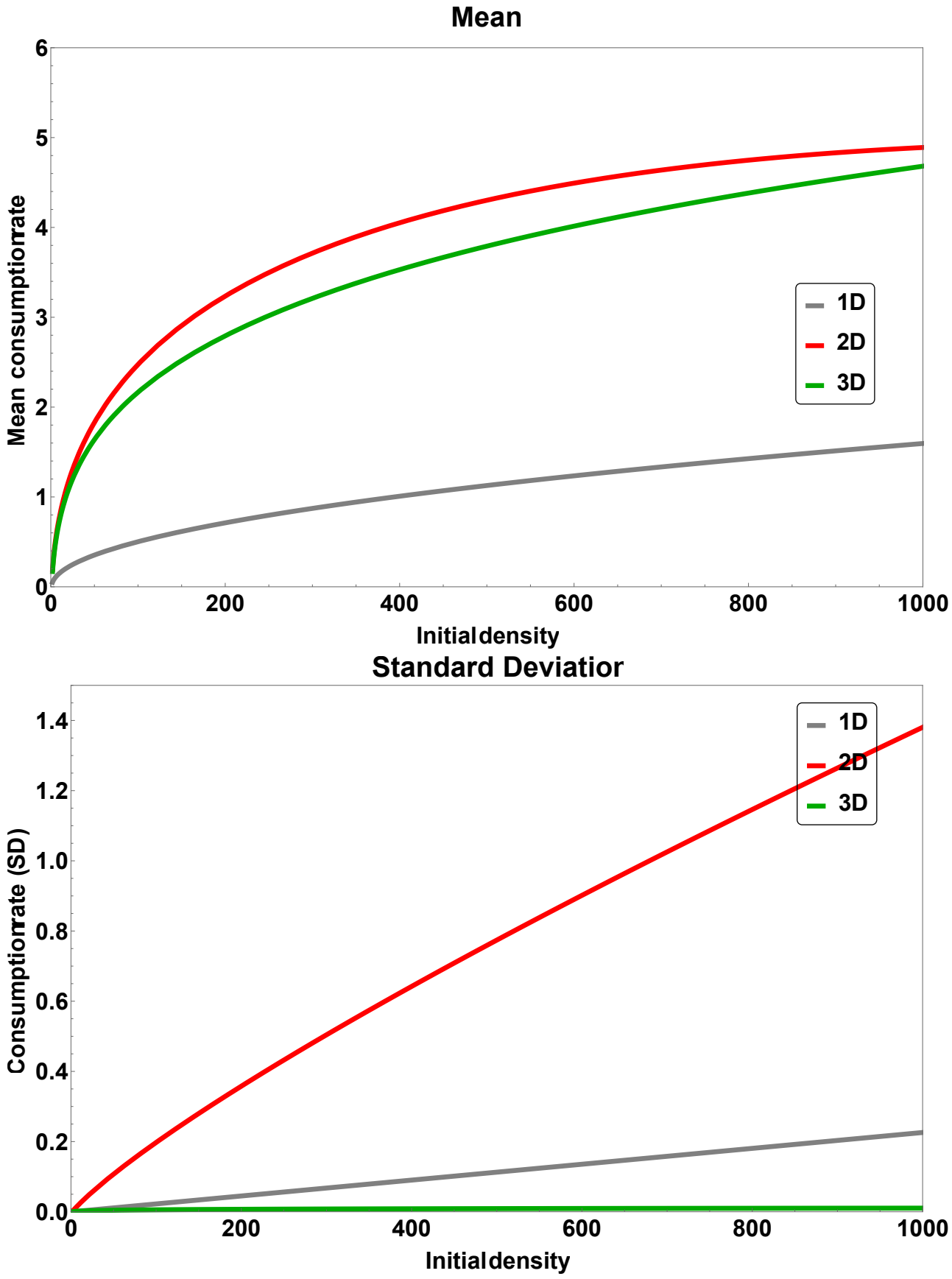

Figure C.1: Illustration of the mean and standard deviation of the consumption rate F_t (parameters: $t = 10^3, \tau_e = 1, \tau_h = 0.045$).

C.2 Coefficient of variation of the consumption rate with between individuals variability

Suppose now that the consumption rate is a random variable which depends on two independent sources of random variations denoted ω_1 and ω_2, such that $F_t(\omega_1, \omega_2) := R_t(\omega_1, \omega_2)/t$. ω_1 is the between-individual variability for searching and handling , *i.e.* parameters involved in searching $\tau_e(\omega_1)$ and handling $\tau_h(\omega_1)$ for a focal individual are randomly chosen in distributions depending on ω_1. The parameters involved in the searching and handling times can have any explicit form (not necessarily Gaussian) but with finite mean and variance. ω_2 is the variability due to the foraging stochastic process itself, *i.e.* the stochastic trajectory of the focal individual when foraging follows a random distribution $\mathcal{W}^{(d)}(\omega_2)$. The distribution $\mathcal{W}^{(d)}(\omega_2)$ followed by the trajectories directly emerges from the assumptions of the foraging process, here the simple random walk in dimension d.

As shown in (C.1), when the foraging time t is large, the distribution of the consumption rate in a d-dimension space after a time t for a focal individual takes the general form

$$F_t^{(d)}(\omega_1, \omega_2) = m_t^{(d)}(\omega_1) + s_t^{(d)}(\omega_1)\mathcal{W}_t^{(d)}(\omega_2) + o_{\mathbb{P}}\left(s_t^{(d)}(\omega_1)\right), \tag{C.2}$$

where $m_t^{(d)}(\omega_1)$ and $s_t^{(d)}(\omega_1)$ are functions which depend on time t, the dimension of space d, and the properties of individuals given by parameters $\tau_h(\omega_1)$ and $\tau_e(\omega_1)$. When these parameters are compactly supported in $(0, \infty)$, the proof of uniform integrability, namely Proposition B.4, can be directly extended, since all bounds are uniform with respect to parameters. We obtain that the mean and variance of the consumption rate satisfy, for $t \to \infty$ (thereafter notations ω_1 and ω_2 are dropped for the sake of simplicity):

$$\begin{aligned}
\mathbb{E}\left[F_t^{(d)}\right] &\sim \mathbb{E}\left[m_t^{(d)}\right] + \mathbb{E}\left[s_t^{(d)}\mathcal{W}^{(d)}\right], \\
\mathrm{Var}\left[F_t^{(d)}\right] &\sim \mathbb{E}\left[\left(m_t^{(d)} + s_t^{(d)}\mathcal{W}^{(d)}\right)^2\right] - \mathbb{E}\left[\left(m_t^{(d)} + s_t^{(d)}\mathcal{W}^{(d)}\right)\right]^2 \\
&\sim \mathbb{E}\left[\left(m_t^{(d)}\right)^2\right] - \mathbb{E}\left[\left(m_t^{(d)}\right)\right]^2 \\
&\quad + \mathbb{E}\left[\left(s_t^{(d)}\mathcal{W}^{(d)}\right)^2\right] - \mathbb{E}\left[\left(s_t^{(d)}\mathcal{W}^{(d)}\right)\right]^2 \\
&\quad + 2\left(\mathbb{E}\left[\left(m_t^{(d)}s_t^{(d)}\mathcal{W}^{(d)}\right)\right] - \mathbb{E}\left[m_t^{(d)}\right]\mathbb{E}\left[s_t^{(d)}\mathcal{W}^{(d)}\right]\right).
\end{aligned}$$

As the sources of variability ω_1 and ω_2 are independent, we have

$$\begin{aligned}
\mathbb{E}\left[s_t^{(d)}\mathcal{W}^{(d)}\right] &= \mathbb{E}\left[s_t^{(d)}\right]\mathbb{E}\left[\mathcal{W}^{(d)}\right], \\
\mathrm{Var}\left[s_t^{(d)}\mathcal{W}^{(d)}\right] &= \mathbb{E}\left[\left(s_t^{(d)}\right)^2\right]\mathrm{Var}\left[\mathcal{W}^{(d)}\right] + \mathrm{Var}\left[s_t^{(d)}\right]\mathbb{E}\left[\mathcal{W}^{(d)}\right]^2.
\end{aligned}$$

In addition, as we have $\mathbb{E}\left[m_t^{(1)}\right] = 0$ and $\mathbb{E}\left[\mathcal{W}^{(2)}\right] = \mathbb{E}\left[\mathcal{W}^{(3)}\right] = 0$ (Eqs. C.1), the expression of the variance of the consumption rate $F_t^{(d)}$ further simplifies to

$$\mathrm{Var}\left[F_t^{(d)}\right] \sim \mathbb{E}\left[\left(m_t^{(d)}\right)^2\right] - \mathbb{E}\left[\left(m_t^{(d)}\right)\right]^2 + \mathbb{E}\left[\left(s_t^{(d)}\mathcal{W}^{(d)}\right)^2\right] - \mathbb{E}\left[\left(s_t^{(d)}\mathcal{W}^{(d)}\right)\right]^2 \tag{C.3}$$

$$\sim \mathrm{Var}\left[m_t^{(d)}\right] + \mathrm{Var}\left[s_t^{(d)}\mathcal{W}^{(d)}\right]. \tag{C.4}$$

Finally, a general expression for the coefficient of variation of the consumption rate is

$$\mathrm{CV}\left[F_t^{(d)}\right] \sim \frac{\sqrt{\mathrm{Var}\left[m_t^{(d)}\right] + \mathrm{Var}\left[s_t^{(d)}\mathcal{W}^{(d)}\right]}}{\mathbb{E}\left[m_t^{(d)}\right] + \mathbb{E}\left[s_t^{(d)}\mathcal{W}^{(d)}\right]}$$

$$\sim \frac{\sqrt{\mathrm{Var}\left[m_t^{(d)}\right] + \mathbb{E}\left[\left(s_t^{(d)}\right)^2\right]\mathrm{Var}\left[\mathcal{W}^{(d)}\right] + \mathrm{Var}\left[s_t^{(d)}\right]\mathbb{E}\left[\mathcal{W}^{(d)}\right]^2}}{\mathbb{E}\left[m_t^{(d)}\right] + \mathbb{E}\left[s_t^{(d)}\right]\mathbb{E}\left[\mathcal{W}^{(d)}\right]}$$

which finally gives (Eqs. C.1)

$$\begin{cases} \mathrm{CV}\left[F_t^{(1)}\right] & \sim \frac{\sqrt{\mathbb{E}\left[\left(s_t^{(1)}\right)^2\right]\mathrm{Var}\left[\mathcal{W}^{(1)}\right] + \mathrm{Var}\left[s_t^{(1)}\right]\mathbb{E}\left[\mathcal{W}^{(1)}\right]^2}}{\mathbb{E}\left[s_t^{(1)}\right]\mathbb{E}\left[\mathcal{W}^{(1)}\right]} = \frac{1}{\mathbb{E}\left[s_t^{(1)}\right]}\sqrt{\mathrm{Var}\left[s_t^{(1)}\right] + \mathbb{E}\left[\left(s_t^{(1)}\right)^2\right]\frac{\mathrm{Var}\left[\mathcal{W}^{(1)}\right]}{\mathbb{E}\left[\mathcal{W}^{(1)}\right]^2}}, \\ \mathrm{CV}\left[F_t^{(2)}\right] & \sim \frac{\sqrt{\mathrm{Var}\left[m_t^{(2)}\right] + \mathbb{E}\left[\left(s_t^{(2)}\right)^2\right]\mathrm{Var}\left[\mathcal{W}^{(2)}\right]}}{\mathbb{E}\left[m_t^{(2)}\right]} = \frac{1}{\mathbb{E}\left[m_t^{(2)}\right]}\sqrt{\mathrm{Var}\left[m_t^{(2)}\right] + \mathbb{E}\left[\left(s_t^{(2)}\right)^2\right]\mathrm{Var}\left[\mathcal{W}^{(2)}\right]}, \\ \mathrm{CV}\left[F_t^{(3)}\right] & \sim \frac{\sqrt{\mathrm{Var}\left[m_t^{(3)}\right] + \mathbb{E}\left[\left(s_t^{(3)}\right)^2\right]\mathrm{Var}\left[\mathcal{W}^{(3)}\right]}}{\mathbb{E}\left[m_t^{(3)}\right]} = \frac{1}{\mathbb{E}\left[m_t^{(3)}\right]}\sqrt{\mathrm{Var}\left[m_t^{(3)}\right] + \mathbb{E}\left[\left(s_t^{(3)}\right)^2\right]\mathrm{Var}\left[\mathcal{W}^{(3)}\right]}. \end{cases}$$

Roughly speaking, the coefficient of variation of the consumption rate $F_t^{(d)}$ is a function of two variance components such as: $c_1\,\mathrm{Var}\left[\omega_1\right] + c_2\,\mathrm{Var}\left[\omega_2\right] + c_3\,\mathrm{Var}\left[\omega_1\right]\mathrm{Var}\left[\omega_2\right]$, where c_1, c_2, c_3 are constants. This shows that if the between-individuals variability has a lower order than the variability of the foraging process itself ($\mathrm{Var}\left[\omega_1\right] \ll \mathrm{Var}\left[\omega_2\right]$), then the coefficient of variation of the consumption rate $\mathrm{CV}\left[F_t\right]$ should be of the same order than the coefficient of variation of the foraging process, *i.e.* of order 1 in 1D, $1/\ln t$ in 2D, or $1/\sqrt{t}$ in 3D. In other words, if the main driver of the variation of the consumption rate is the foraging process itself, then the coefficients of variation estimated from data should be at most of order 1 (or more precisely it should fall within the range given in Tab. 1). If its order of magnitude is larger than 1 (or more precisely if it falls outside the range given in Tab. 1), then we could conclude that the main driver of the variation of the consumption rate is the between-individual variability (*i.e.* $\mathrm{Var}\left[\omega_1\right] \gg \mathrm{Var}\left[\omega_2\right]$).

Two other alternatives are possible, yet less plausible. First, the coefficient of variation estimated from data could be of order lower than 1, which would mean that both the between-individual variability and the variability due to the foraging process itself are of order lower than 1. Second, the coefficient of variation estimated from data could be of order 1 and at the same time the between-individual variability be of order larger than the variability

from the foraging process. If so, it would remain to explain how it is possible that the between-individual variability is such that the coefficient of variation falls exactly in this order of magnitude. Those two alternatives would seem even less plausible when the estimated coefficients of variation cover a large number of species and experimental and ecological contexts, as in our case and the datasets we compiled.

Therefore, we finally make two global predictions: either the coefficients of variation estimated from data are at most of order 1, or they are of order larger than 1. We would then conclude that the main driver of the variation of the consumption rate is the foraging process in the former case, or that it is external sources of variations, such as the between-individual variability, in the latter.

D Stochastic simulations

D.1 Standard setup

We first evaluated the accuracy and the convergence rate of the approximation of $CV_t^{(d)}$, the coefficient of variation of the consumption rate, defined as the number of prey per unit of time consumed by a predator foraging in a d-dimensional space during a total foraging duration t.

To achieve this, we conducted numerical stochastic simulations of a consumer randomly and symmetrically walking on a d-dimensional homogeneous square lattice where each node initially contains a prey (Fig. D.1). The consumer moves from one node to any of the four other adjacent nodes at constant speed v. When a node with a prey is encountered, the consumer feeds on the prey, which takes a constant handling time τ_h, and the node is depleted (we assume there is no regeneration of the prey). If the node was already visited, the consumer randomly moves to any of the adjacent node without spending handling time on the currently visited node.

Denoting x the initial density of prey in the lattice, and L an arbitrary length unit, the distance between two prey in the lattice is

$$y^{(d)}(x) = \frac{L}{x^{1/d} - 1}. \tag{D.1}$$

The time to cover this distance is then given by $\tau_e^{(d)}(x) = y^{(d)}(x)/v$. A simulation run (i.e. one trajectory or realization of the stochastic process) is stopped when the total foraging duration t is reached, time at which the total number of prey consumed $R_t^{(d)}(x)$ is counted, and the consumption rate $F_t^{(d)}(x) = R_t^{(d)}(x)/t$ is recorded. 10^4 realizations per initial density x were run with the following parameters values: $t = 10^7$, $v = 1$, $\tau_h = 0.1$, $L = 1000$.

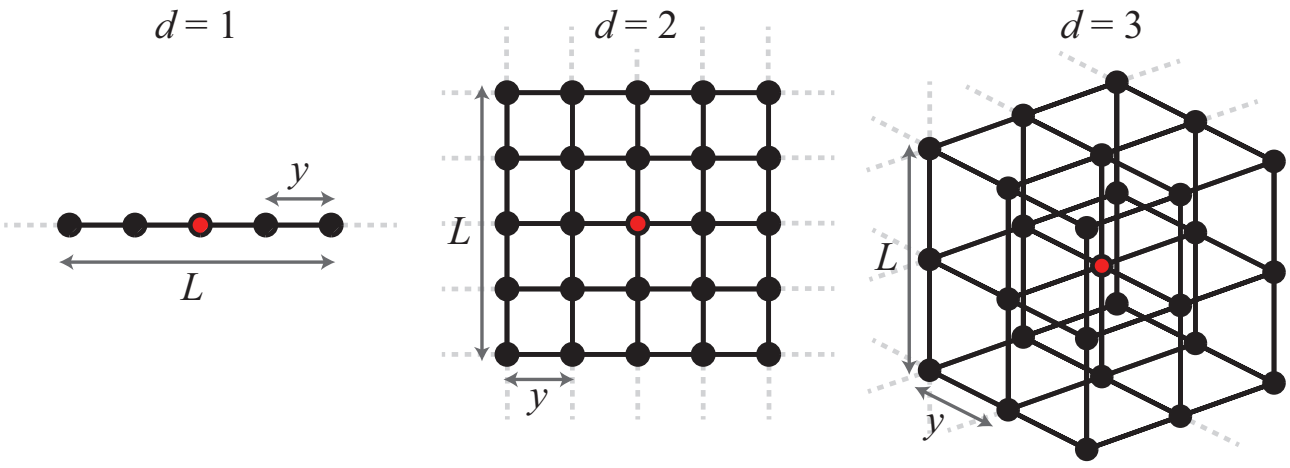

Figure D.1: Illustration of the lattice for $d = \{1, 2, 3\}$. The red dot denotes the starting position of the walker. L is an arbitrary length unit; y is the distance between two nodes; d is the dimension of space.

D.2 Robustness

We evaluated, under various ecological contexts, the robustness of the analytical approximations of $CV_t^{(d)}$, the coefficient of variations of the consumption rate. We ran numerical stochastic simulations of modified versions of the standard algorithm described in the previous section. Specifically, we ran simulations with one the four following additional mechanisms (detailed below): Walk with stochastic length jumps, walk with drift, self-avoiding walk, and walk in an initially heterogeneous and random repartition of prey on the lattice.

Jumps with random length. The consumer moves in the lattice following a symmetrical random walk with jumps of length following a truncated power-law distribution $P(k) \sim k^{-\theta}$ with $k \in [1, k_{\max}]$, where $k_{\max}$ is the maximum step-size. Simulations were run for the following parameter values: $\theta \in \{2.0, 2.5, 3.0, 3.5\}$, $k_{\max} = 10$. Other parameters were the same than in the standard setup (see previous section).

Walk with drift. The consumer moves on the lattice in a preferred direction, denoted $\rightarrow$. The drift parameter $\mu \in [0, 1]$ is defined such that, each step, the consumer has the probability

$$\mathbb{P}(\text{jump} =' \rightarrow') = \frac{1 + (2d-1)\mu}{2d}$$

to move in this preferred direction, and a probability

$$\mathbb{P}(\text{jump} \neq' \rightarrow') = \frac{1 - \mu}{2d}$$

to move in any of the $2d - 1$ remaining directions: $\leftarrow$ in 1D, $\leftarrow$, $\downarrow$ or $\uparrow$ in 2D, $\leftarrow$, $\downarrow$ or $\uparrow$, $+1\,level$ or $-1\,level$ in 3D. If $\mu = 0$ the movement is symmetrical and resumes to the standard random walk. If $\mu = 1$, the movement is unidirectional. Simulations were run with following parameter values, corresponding to an increasing biased random walk $\mu \in \{0.05, 0.1, 0.25, 0.5\}$.

Self-avoiding walk with a short term memory. The consumer had a short-term memory avoiding the node it just left.

Walk on a lattice with a random initial repartition of prey. Each node of the lattice initially contains a prey with probability p. In practice, each time the consumer visited an unvisited node, a Bernoulli trial with probability p were drawn. If $p = 1$, the walk resumes to a typical random walk on a uniform graph (as detailed in the previous section), if $p = 0$ the lattice is initially empty. By default simulations were run for $p = 1/2$, unless indicated.

E Data

N.B.: All data, associated papers (when available) and R scripts are available on the following server: github.

E.1 Dataset 1: FoRAGE database

The first dataset was obtained from the database FoRAGE [15], dowloaded from https://knb.ecoinformatics.org/ in january 2021 (version 12.18.18). The database contains the predator and prey species names, the literature source, the initial prey density (either per m^2 or m^3), the consumption rate (the number of prey eaten per day per predator), the sample size per treatment (i.e. the initial density). The database FoRAGE was partly built by automatically extracting data from papers' figures, and partly populated directly from tables (see [15] for details). We discarded all data where at least one of these information was missing.

There were two categories of available data that were differently used for the calculation of the coefficient of variation estimations: i) raw data or ii) summary statistics. In the case of i) raw data: because there could have overlaps between dots in figures (i.e. when different predators fed on the same number of prey), the number of data could be lower than the sample size announced in the initial paper, in particular when the initial density of prey was low. We thus curated the database by removing the data with too large uncertainty: we only kept data where the sample size was ≥ 8 and where the number of available measured consumption rate was at least 80% of the sample size (i.e. at least 8 data points if the sample size was 10, for example). In addition, when a single dot was detected from the figure for a given experimental treatment, the FoRAGE's authors filled the database with a single value for as many independent replicates as supposed from the methods described in the original paper (for example, if the sample size was $n = 10$ but a single dot in a figure was observed, the database was populated with 10 rows, one for each replicate, with the same number of eaten prey). As a consequence, there was no variation in the consumption rate in this case but with no certainty about whether it was due to the limit of data collection itself or because there was indeed no variation. We thus decided to exclude these data when there was no variation. The coefficients of variation were estimated by calculating the mean and the standard deviation within initial density directly from raw data. This resulted in 142 estimated coefficients of variation (calculated on 1266 from 15108 initial data after curation), for 19 predator and 17 prey species.

In the case of ii) summary statistics: we only kept data where the mean, the standard error and the sample size were available, where the sample size was ≥ 8 (to ensure minimal quality for summary statistics estimations and be consistent with case i) raw data), and where the standard error was > 0 (because there was uncertainty whether it was true or false zero, and because a standard error equal to 0 was mostly encountered in low densities treatments suggesting that all prey were eaten in all replicates). We calculated the coefficients of variation directly from the mean, standard error and sample size, within an initial density, by applying the formula of the definition of the standard error: $\sigma = \sqrt{n}\ se$ (where n is the sample size, σ is the standard deviation, and se is the standard error;

n and se are given in the database). This resulted in 3039 estimated coefficients of variation aftr curation (from 6797 estimated mean and se consumption rates in total in the database), for 126 predator and 104 prey species.

Overall the coefficients of variation calculated from data compiled in the FoRAGE database may contain the following sources of variations: i) between individuals; ii) within individuals (if different or identical individuals were used for a given initial density or for different initial densities, information not available from the database); iii) between environments, as it was not known to what extent the environmental conditions of the experiment were controlled; iv) experimental and observations errors; v) errors due to the FoRAGE database build itself (in particular due to the automatic image analysis and data collection); vi) from the foraging process itself.

Fig. E.1 shows the median and quartiles of all the coefficients of variation calculated from the FoRAGE database. The median is 0.2905. 73.2% of the coefficients of variation lie between 0.1 and 1, and 95.5% lie between 0.01 and 10.

E.2 Dataset 2: Raw data, potentially entangled between- and within- individuals variations

The datasets were obtained from

- The Dryad deposit (search in january 2021 with keywords: "foraging", "intake", "functional response", "visitation rate", 15 collected datasets).
- The database by [16] available at `github.com/stoufferlab/general-functional-responses` (25 datasets). From this database, we extracted and used only datasets where the number of predators was fixed to one, where there was several measurements at a given density, and a single type of prey; we excluded any dataset where inconsistencies were detected or with uncertainties; we included datasets where the mean, the sample size and the standard errors were available, from which we calculated the coefficients of variation.
- Data from direct authors sharing. We directly contacted authors for data sharing (1 dataset from [17].

Overall we computed 602 coefficients of variation from 41 different datasets (from which 20 coefficients of variation were equal to 0, all in the case of low densities: suggesting that all prey were consumed by all predators, resulting in a standard deviation equal to 0; As the minimum non-zero value of the coefficient of variation was ≥ 0.029, we discarded zero values). The coefficients of variation calculated from these datasets potentially contains the following sources of variations: i) between individuals; ii) within individuals (if different or identical individuals were used for a given initial density or for different initial densities, information not available from the database by [16], or with uncertainty from datasets downloaded from Dryad, or the dataset shared by the author); iii) between environments, as it was not known to what extent the environmental conditions of the experiment were controlled; iv) experimental and observations errors; v) the foraging process itself.

Fig. E.1 shows the median and quartiles of all the coefficients of variation calculated from these raw datasets. The median is 0.408, 87.8% of the coefficients of variation lie between 0.1 and 1, and 100% lie between 0.01 and 10.

List of references: Data obtained directly from the authors: [17]. Data obtained from Dryad deposit: [18, 19, 20, 21, 22, 23, 24, 25, 26, 27, 28, 29, 30, 31, 32]. Data from the database: [16].

E.3 Dataset 3: Raw data, accounting for within individuals variations

We collected three datasets directly from the authors where consumption rates were measured several times for the same individuals. One dataset were obtained in natural conditions [33], in semi-natural conditions [34], or in controlled conditions [35]. We directly calculated coefficients of variation within individuals from the raw data shared by [33] and [35]. The coefficients of variation were calculated by the authors themselves and shared with us in the case of the Imperial shag [34]. It resulted in 229 estimations of within-individuals coefficients of variation. In natural and semi-natural conditions, the sources of possible variations were: i) within individuals; ii) the environment (including uncontrolled prey densities); iii) experimental errors, iv) the foraging process itself. In the controlled conditions, the sources of possible variations were: i) within individuals; ii) experimental errors; iii) the foraging process itself. In the case of the crayfish experiments [35], we could calculate the coefficients of variation within individuals within and across densities as the same individuals were used several times for a given density, and for different densities.

Fig. E.1 shows the median and quartiles of all the coefficients of variation calculated from these datasets. The median is 0.273, 85.1% of the coefficients of variation lie between 0.1 and 1, and 99.1% lie between 0.01 and 10.

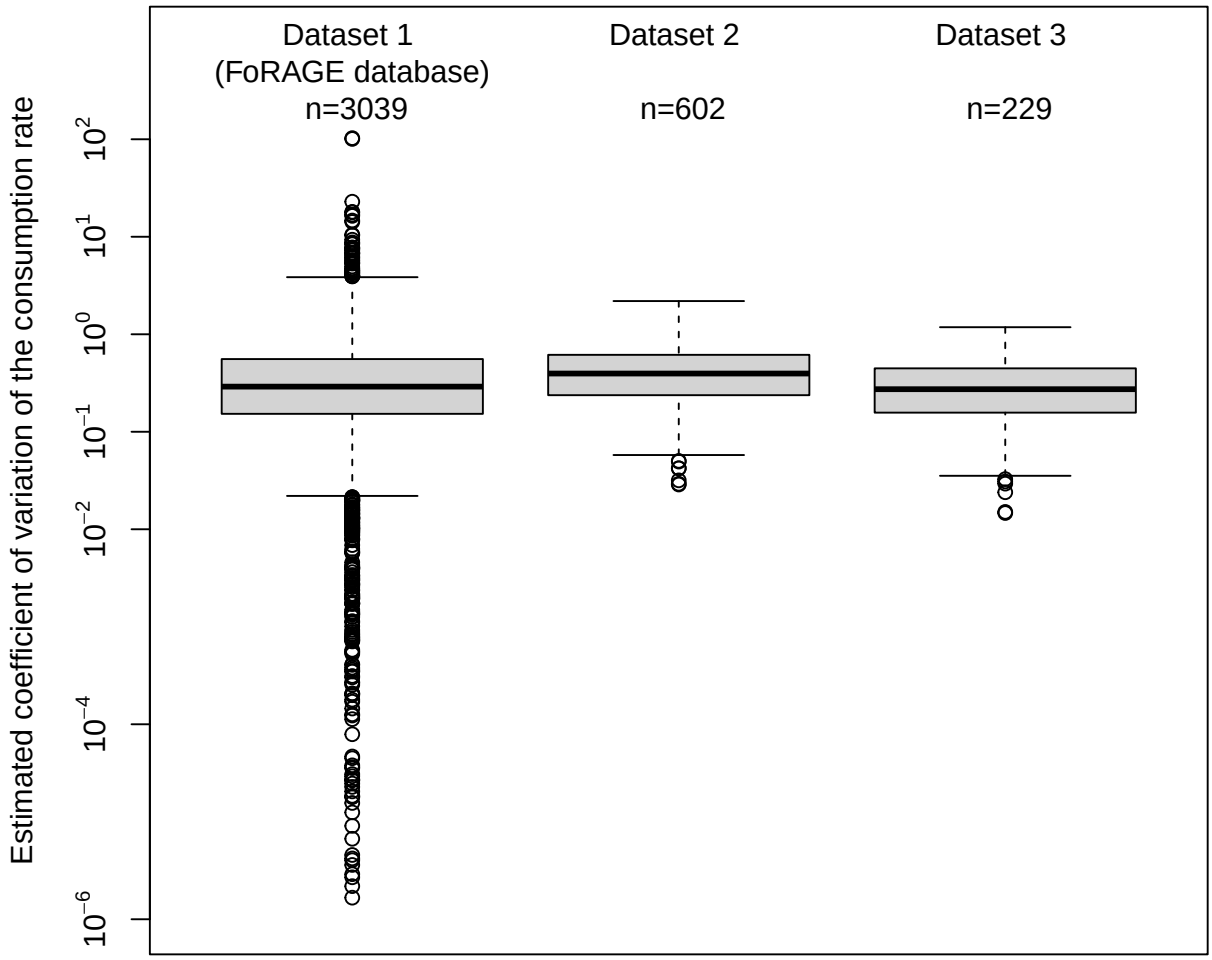

Figure E.1: Boxplot of the coefficients of variation of the consumption rate of prey per single predator calculated from different datasets (see text for details).

References

[1] Frank Spitzer. Principles of random walk, volume 34. Springer Science & Business Media, 2001.

[2] Aryeh Dvoretzky and Paul Erdös. Some problems on random walk in space. In Proceedings of the second Berkeley symposium on mathematical statistics and probability, volume 2, pages 353–368. University of California Press Berkeley and Los Angeles, 1951.

[3] Yoshinori Nagai, Hiroshi Asai, and Takashi Tsuchiya. The average number of distinct sites visited by a one-dimensional random walker and its application to isotope exchange in polypeptides. Biophysical Chemistry, 13(3):213–222, 1981.

[4] William Feller. The asymptotic distribution of the range of sums of independent random variables. The Annals of Mathematical Statistics, pages 427–432, 1951.

[5] Naresh C Jain and William E Pruitt. The range of random walk. In Proceedings of the Sixth Berkeley Symposium on Mathematical Statistics and Probability (Univ. California, Berkeley, Calif., 1970/1971), volume 3, pages 31–50, 1972.

[6] Kôhei Uchiyama. The first hitting time of a single point for random walks. Electronic Journal of Probability, 16:1960–2000, 2011.

[7] Enrico Masina. Useful review on the exponential-integral special function. arXiv preprint arXiv:1907.12373, 2019.

[8] J-F Le Gall. Propriétés d'intersection des marches aléatoires. Communications in mathematical physics, 104(3):471–507, 1986.

[9] Jean-François Le Gall. Sur le temps local d'intersection du mouvement brownien plan et la méthode de renormalisation de varadhan. In Séminaire de Probabilités XIX 1983/84, pages 314–331. Springer, 1985.

[10] Richard F Bass, Xia Chen, and Jay Rosen. Moderate deviations for the range of planar random walks. American Mathematical Soc., 2009.

[11] Patrick Billingsley. Convergence of probability measures. John Wiley & Sons, 2013.

[12] Naresh C Jain and William E Pruitt. The range of transient random walk. Journal d'Analyse Mathématique, 24(1):369–393, 1971.

[13] Gregory F Lawler and Vlada Limic. Random walk: a modern introduction, volume 123. Cambridge University Press, 2010.

[14] Naresh Jain and Steven Orey. On the range of random walk. Israel Journal of Mathematics, 6:373–380, 1968.

[15] Stella F. Uiterwaal, Ian T. Lagerstrom, Shelby R. Lyon, and John P. DeLong. Forage database: A compilation of functional responses for consumers and parasitoids. Ecology, 103(7):e3706, 2022.

[16] Mark Novak and Daniel B Stouffer. Systematic bias in studies of consumer functional responses. Ecology Letters, 24(3):580–593, 2021.

[17] D.J. Baker, R.A. Stillman, B.M. Smith, J.M. Bullock, and K.J. Norris. Vigilance and the functional response of granivorous foragers. Functional Ecology, 24:1281–1290, 2010.

[18] Corey J Thorp, Mhairi E Alexander, James R Vonesh, and John Measey. Size-dependent functional response of xenopus laevis feeding on mosquito larvae. PeerJ, 6:e5813, 2018.

[19] Sjoerd Duijns, Ineke E Knot, Theunis Piersma, and Jan A van Gils. Field measurements give biased estimates of functional response parameters, but help explain foraging distributions. Journal of Animal Ecology, 84(2):565–575, 2015.

[20] Austin J Gallagher, Simon J Brandl, and Adrian C Stier. Intraspecific variation in body size does not alter the effects of mesopredators on prey. Royal Society Open Science, 3(12):160414, 2016.

[21] Berith B Bressendorff and Søren Toft. Dome-shaped functional response induced by nutrient imbalance of the prey. Biology Letters, 7(4):517–520, 2011.

[22] Daniel Barrios-O'Neill, Jaimie TA Dick, Mark C Emmerson, Anthony Ricciardi, and Hugh J MacIsaac. Predator-free space, functional responses and biological invasions. Functional Ecology, 29(3):377–384, 2015.

[23] Stella F Uiterwaal, Anthony I Dell, and John P DeLong. Arena size modulates functional responses via behavioral mechanisms. Behavioral Ecology, 30(2):483–489, 2019.

[24] Ryan J Wasserman, Mhairi E Alexander, Tatenda Dalu, Bruce R Ellender, Horst Kaiser, and Olaf LF Weyl. Using functional responses to quantify interaction effects among predators. Functional Ecology, 30(12):1988–1998, 2016.

[25] Arnaud Sentis, Julie Morisson, and David S Boukal. Thermal acclimation modulates the impacts of temperature and enrichment on trophic interaction strengths and population dynamics. Global Change Biology, 21(9):3290–3298, 2015.

[26] Olivera Vucic-Pestic, Björn C Rall, Gregor Kalinkat, and Ulrich Brose. Allometric functional response model: body masses constrain interaction strengths. Journal of Animal Ecology, 79(1):249–256, 2010.

[27] Benjamin J Toscano and Blaine D Griffen. Trait-mediated functional responses: predator behavioural type mediates prey consumption. Journal of Animal Ecology, 83(6):1469–1477, 2014.

[28] Ana Born-Torrijos, Rachel A Paterson, Gabrielle S van Beest, Jessica Schwelm, Tereza Vyhlídalová, Eirik H Henriksen, Rune Knudsen, Roar Kristoffersen, Per-Arne Amundsen, and Miroslava Soldánová. Temperature does not influence functional response of amphipods consuming different trematode prey. Parasitology Research, 119:4271–4276, 2020.

[29] Monica McCard, Josie South, Ross N Cuthbert, James WE Dickey, Nathan McCard, and Jaimie TA Dick. Pushing the switch: functional responses and prey switching by invasive lionfish may mediate their ecological impact. Biological invasions, 23(6):2019–2032, 2021.

[30] Nan Hu, Yajuan Huang, Zhenglin Yu, Tao Zhang, Dapeng Liu, and Marcus Lee. Handling-or digestion-limited predators: the role of body mass and habitat complexity in predator functional response. Marine Ecology Progress Series, 725:1–14, 2023.

[31] Ross N Cuthbert, Syrmalenia G Kotronaki, Jasmin C Hütt, Elisabeth Renk, Niklas Warlo, and Elizabeta Briski. Do alternative resources dampen functional responses of native but not alien gammarids? Ecology and Evolution, 12(9), 2022.

[32] Julien Mocq, Pavel R Soukup, Joacim Näslund, and David S Boukal. Disentangling the nonlinear effects of habitat complexity on functional responses. Journal of Animal Ecology, 90(6):1525–1537, 2021.

[33] Yuuki Y. Watanabe, Kentaro Ito, Nobuo Kokubun, and Akinori Takahashi. Foraging behavior links sea ice to breeding success in antarctic penguins. Science Advances, 6(26):eaba4828, 2020.

[34] Rory P Wilson, Mark D Holton, Andrew Neate, Monserrat Del Caño, Flavio Quintana, Ken Yoda, and Agustina Gómez-Laich. Luck and tactics in foraging success: The case of the imperial shag. Marine Ecology Progress Series, 682:1–12, 2022.

[35] Stefan M Linzmaier and Jonathan M Jeschke. Towards a mechanistic understanding of individual-level functional responses: Invasive crayfish as model organisms. Freshwater Biology, 65(4):657–673, 2020.